



Contents lists available at ScienceDirect

Quaternary Science Reviews

journal homepage: www.elsevier.com/locate/quascirev

Late Pleistocene raised beaches of coastal Estremadura, central Portugal

Michael M. Benedetti^{a,*}, Jonathan A. Haws^b, Caroline L. Funk^c, J. Michael Daniels^d, Patrick A. Hesp^e, Nuno F. Bicho^f, Thomas A. Minckley^g, Brooks B. Ellwood^h, Steven L. Formanⁱ^a Department of Geography and Geology, University of North Carolina Wilmington, 601 South College Road, Wilmington, NC 28403, USA^b Department of Anthropology, University of Louisville, Louisville, KY 40292, USA^c 6736 Columbus Avenue, Richfield, MN 55423, USA^d Department of Geography, University of Denver, 2050 East Iliff Avenue, Denver, CO 80208, USA^e Department of Geography and Anthropology, Louisiana State University, Baton Rouge, LA 70803, USA^f Faculdade de Ciências Humanas e Sociais, Universidade do Algarve, Campus de Gambelas, 8005-139 Faro, Portugal^g Department of Botany, University of Wyoming, 1000 East University Avenue, Laramie, WY 82071, USA^h Department of Geology and Geophysics, Louisiana State University, Baton Rouge, LA 70803, USAⁱ Department of Earth and Environmental Sciences, University of Illinois at Chicago, 845 West Taylor Street, Chicago, IL 60607, USA

ARTICLE INFO

Article history:

Received 6 May 2009

Received in revised form

29 September 2009

Accepted 29 September 2009

ABSTRACT

We present new stratigraphic, sedimentological, and chronological data for a suite of tectonically raised beaches dating to Marine Isotope Stages 5, 4, and 3 along the Estremadura coast of west-central Portugal. The beach deposits are found in association with ancient tidal channels and coastal dunes, pollen bearing mud and peat, and Middle Paleolithic archaeological sites that confirm occupation of the coastal zone by Neanderthal populations. The significance of these deposits is discussed in terms of the archaeological record, the tectonic and geomorphic evolution of the coast, and correlation with reconstructions of global climate and eustatic sea-level change. Direct correlation between the Estremadura beach sections is complicated by the tectonic complexity of the area and the age of the beach deposits (which are near or beyond the limit of radiocarbon dating). Evidence from multiple sites dated by AMS radiocarbon and optical luminescence methods suggests broad synchronicity in relative sea-level changes along this coast during Marine Isotope Stage 3. Two beach complexes with luminescence and radiocarbon age control date to about 35 ka and 42 ka, recording a rise in relative sea level around the time of Heinrich Event 4 at 39 ka. Depending on assumptions about eustatic sea level at the time they were deposited, we estimate that these beaches have been uplifted at rates of 0.4–4.3 mm yr⁻¹ by the combined effects of tectonic, halokinetic, and isostatic processes. Uplift rates of 1–2 mm yr⁻¹ are likely if the beaches represent sea level stands at roughly 40 m below modern, as suggested by recent eustatic sea level reconstructions. Evidence from coastal bluffs and the interior of the study area indicates extensive colluvial, fluvial, and aeolian sedimentation beginning around 31 ka and continuing into the Holocene. These geomorphic adjustments are related to concomitant changes in climate and sea level, providing context that improves our understanding of Late Pleistocene landscape change and human occupation on the western Iberian margin.

© 2009 Elsevier Ltd. All rights reserved.

1. Introduction

Late Quaternary climatic instability and its impacts have become major research topics in Quaternary science. High-resolution isotopic records from ice cores and deep-sea sediment cores are

yielding new insights into global climate dynamics and providing important context within which to interpret local geological, archaeological, and paleobotanical phenomena (Imbrie et al., 1984; Bond et al., 1993; GRIP Members, 1993, 2004; Grootes et al., 1993; Bender et al., 1994; van Andel and Tzedakis, 1996; Shackleton et al., 2004). Recently attention has been focused on dramatic environmental changes during Marine Isotope Stage 3 (MIS 3), the period between roughly 60,000 and 25,000 years ago (60–25 ka) (Shackleton et al., 2000; Barron and Pollard, 2002; Huntley et al., 2003; Huber et al., 2006; Vautravers and Shackleton, 2006; Rohling et al., 2008). Climate fluctuations during MIS 3 are evident in proxy temperature records from the Greenland ice sheet; they involve

* Corresponding author. Tel.: +1 910 962 7650; fax: +1 910 962 7077.

E-mail addresses: benedettim@uncw.edu (M.M. Benedetti), jonathan.haws@louisville.edu (J.A. Haws), carolinelfunk@gmail.com (C.L. Funk), j.michael.daniels@du.edu (J.M. Daniels), pahesp@lsu.edu (P.A. Hesp), nbicho@ualg.pt (N.F. Bicho), Minckley@uwyo.edu (T.A. Minckley), ellwood@lsu.edu (B.B. Ellwood), slf@uic.edu (S.L. Forman).

rapid shifts between fully glacial and nearly interglacial conditions preceding the last glacial maximum (Bond et al., 1993; Dansgaard et al., 1993). These fluctuations have been identified in paleo-environmental records in Europe and around the North Atlantic region. Records of MIS 3 climate change, and consequent changes in sediment and pollen delivery to the coast, are evident in deep-sea sediment cores off Portugal (de Abreu et al., 2003; Roucoux et al., 2005; Vautravers and Shackleton, 2006; Daniau et al., 2007). Coordinated efforts such as the Stage Three Project and INTIMATE are working towards correlation of the various paleoenvironmental records and are investigating the landscape-scale impacts of MIS 3 climate variability (Walker et al., 2001; van Andel, 2002).

MIS 3 environmental change in Europe is contemporaneous with the decline of Neanderthal populations and their replacement by anatomically Modern humans at the end of the Middle Paleolithic between roughly 40 and 25 ka (Bicho, 1993; Van Andel and Tzedakis, 1996; Finlayson et al., 2006). Neanderthals occupied Iberia for over 200,000 years until their replacement by anatomically modern humans shortly before the last glacial maximum. Significant debate surrounds the question of whether the extinction was due to habitat change, competition from Moderns, or changes in diet and subsistence patterns (Straus and Bicho, 2000; d'Errico and Sánchez-Goñi, 2003; Hockett and Haws, 2005; Finlayson et al., 2006; Jiménez-Espejo et al., 2007). The use of coastal resources is now at the center of this debate, which has broadened to include questions about eustatic sea-level changes and the productivity of the continental shelves during the late Pleistocene (Finlayson, 2008; O'Regan, 2008). It has also prompted reconsideration of the Broad Spectrum Revolution concept, which held that aquatic resources were not intensively harvested until forced by reductions in terrestrial game at the end of the Pleistocene (Erlandson, 2001; Stiner, 2001). These questions are driving new paleoenvironmental studies of MIS 3 with an increased interest in coastal ecology and geodynamics during this period.

The impacts of MIS 3 climate change on coastal systems, including the magnitude and timing of eustatic sea-level changes, are probably large but are poorly understood (Chappell et al., 1996; Rohling et al., 2008; Siddall et al., 2008). Time-averaging involved in deep-sea sediment and coral reef records leads to concerns about short-lived events that may have important local impacts but may not be recorded in these archives. Meanwhile, direct stratigraphic evidence of coastal change is fragmentary and complicated by local tectonic, glacio-isostatic, and hydro-isostatic adjustments. These problems are amplified for coastal changes during MIS 3, because postglacial transgression has eroded or inundated the evidence along most coastlines, and because of newly documented problems with radiocarbon calibration before about 30 ka (Fairbanks et al., 2005; Weninger and Jöris, 2008). Other dating methods available for MIS 3 coastal deposits (amino acid racemization, optical luminescence, uranium-series dating) can be subject to relatively large analytical uncertainties. Numerous studies have addressed coastal geomorphic change in western Europe during MIS 3, but the evidence is scarce and correlation between sites remains problematic (in addition to those discussed below, see Clemmensen et al., 2001; Whittington and Hall, 2002; Rodríguez-Vidal et al., 2004).

This study presents stratigraphic evidence from previously undocumented and undated raised beach deposits in west-central Portugal. The evidence includes lithologic descriptions and chronostratigraphic correlation of the raised beach sections, with facies associations supported by sedimentological data. We also present complementary geomorphic and paleobotanical information, and a summary of new archaeological finds in the study area. The results add significantly to what is known about relative sea-level change, neotectonic activity, early human occupation, and

paleobotanical change on the central Portuguese coast. They also allow us to begin untangling the influences of relative sea-level change and climate change in driving the geomorphic evolution of this coastline.

2. Regional setting

The study area is the northern portion of the Estremadura coast in central Portugal between roughly 39 and 40 N latitude (Fig. 1). It is a high-relief bedrock coast where tectonic stresses have produced a diverse assemblage of rocky headlands, protected bays, fault-strike valleys, and uplifted bedrock platforms along the coast. North of Nazaré, the study area is covered by a rolling sand plain that extends 10–15 km inland; to the south, isolated dune fields fill gaps in the coastal bluffs. Tides are semidiurnal with a mean spring tidal range of 2.9 m (Dinis et al., 2006). The coast is exposed to the high-energy swells and storm waves from the northwest that are generated in the high-latitude North Atlantic Ocean. Wave characteristics include significant wave height of 1–3 m and period of 9–13 s (>50% frequency), while frequent winter storms bring wave heights above 10 m (Ferreira et al., 2008). North of the cliffs at Nazaré, the beach is influenced by strong longshore drift southward from fluvial sources including the Rio Lis and Rio Mondego. South of Nazaré, sediment sources are local and beaches are narrow or absent. Wave erosion during winter storms is causing rapid retreat of the coastal bluffs, exposing the stratigraphic sections described in this paper.

Tectonics in the study area are governed by the interplay between a set of strike-slip faults, thrust faults, and salt diapirs (Fig. 2). The study area is roughly bisected by the Nazaré fault, a major transfer fault aligned with a submarine canyon immediately offshore. North of the Nazaré fault, the Monte Real Cenozoic Basin is composed mainly of continental siliciclastic rocks. The southern part of the study area comprises the NNE–SSW trending Lusitanian Basin, a Mesozoic rift basin associated with the opening of the Tethys seaway (Pinheiro et al., 1996; Azeredo et al., 2002). Rocks of the Lusitanian Basin are mostly Jurassic platform carbonates and Cretaceous siliciclastics. The bounding faults of the Lusitanian Basin have been reactivated under a compressive–transpressive regime during the Cenozoic convergence of North Africa with Iberia. Northwestward motion of Africa at 4–5 mm yr⁻¹ is responsible for significant crustal deformation, up to 1000 m of uplift since the early Pliocene, and movement along strike-slip and thrust faults in central Portugal (Rasmussen et al., 1998; Cloetingh et al., 2005; Cunha et al., 2005).

Throughout the study area are salt diapirs generated by massive evaporite deposition in an isolated part of the Tethys seaway during the Late Triassic and Early Jurassic (Alves et al., 2003). The diapirs form structural anticlines where Jurassic and Cretaceous beds, often steeply dipping or strongly deformed, are exposed at the surface. The largest of these is the Caldas da Rainha structure (Fig. 2), a 40-km long valley oriented parallel to the modern coast produced by unroofing along the axis of the diapir. The interior of the Caldas diapir contains at least 30 m of Pleistocene and Holocene alluvial fill (Henriques and Dinis, 2006). Valleys cut into this fill during the last glacial maximum were flooded to form a series of inland lagoons during the Holocene (Dinis et al., 2006). These and several other structurally controlled lagoons along the Portuguese margin share a similar Late Pleistocene history of trenching during the glacial maximum, flooding during the Early Holocene, and partial infilling by historical sedimentation (Boski et al., 2002; Freitas et al., 2003; Cabral et al., 2006). Gentle synclines associated with salt withdrawal into the diapirs influence the coastal sections north of Nazaré and south of Foz do Arelho.

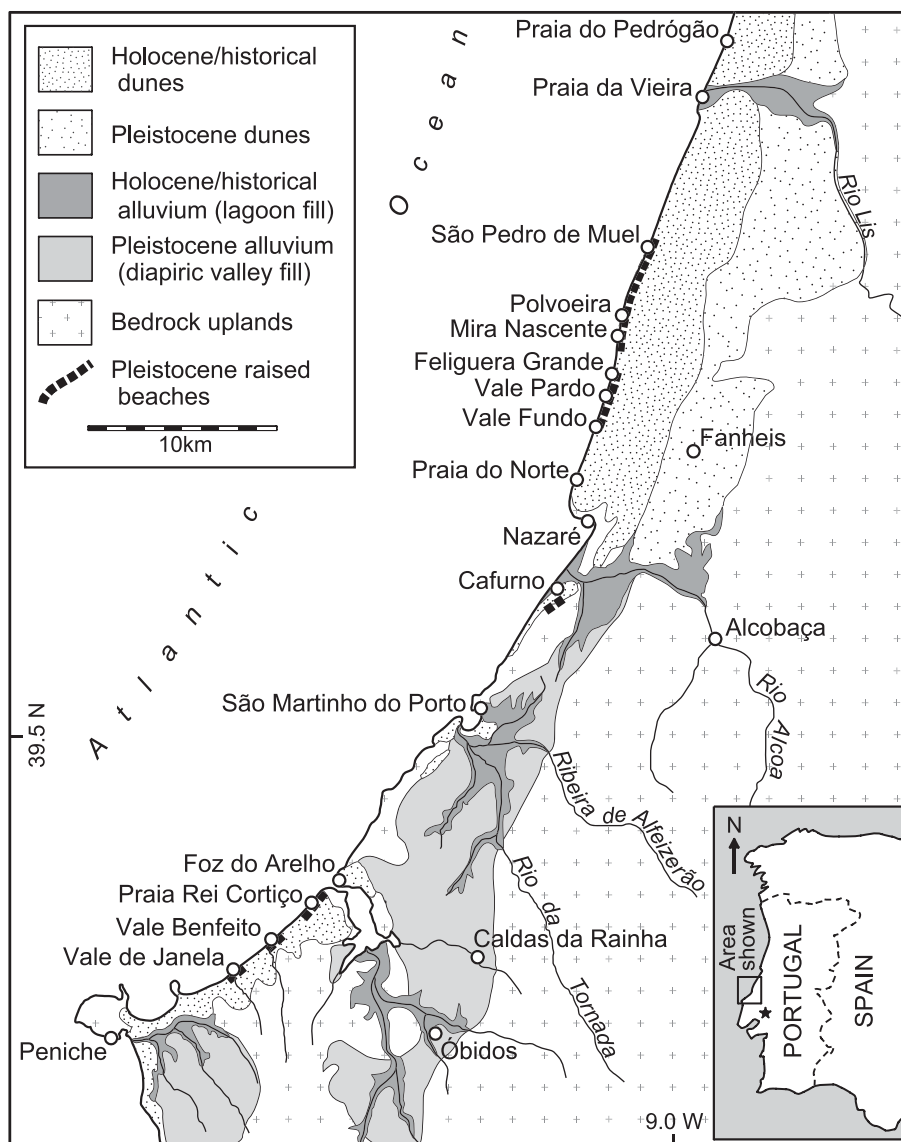


Fig. 1. Map of the northern Estremadura coast, showing geomorphic features and locations discussed in the text. Geological boundaries adopted from França and Zbyszewski (1963).

Neotectonic activity in western Iberia is associated with the continued tectonic evolution of the region from passive to active margin. Evidence for neotectonic activity includes widespread deformation of Pleistocene strata and historical seismicity (Cabral and Ribeiro, 1989; Ferreira, 1991; Granja, 1999; Maldonado and Nelson, 1999; Zitellini et al., 2004; Abrantes et al., 2005; Pereira et al., 2007; Cunha et al., 2008). Some workers have cautioned that many of these features could have a sediment-loading or karst origin (Dias and Cabral, 2002; Dinis et al., 2007). Neotectonics have been instrumental in uplifting and preserving Late Pleistocene coastal deposits and archaeological sites along much of the Estremadura coastline (Breuil and Zbyszewski, 1945; Zbyszewski, 1971). Bluff-top deposits in the study area between Vale Pardo and São Pedro de Muel were mapped as Pleistocene by França and Zbyszewski (1963), but these sections have not previously been dated or described in detail. Firtion and Carvalho (1952) examined a raised beach deposit in the coastal bluffs at São Pedro de Muel, reporting particle size and pollen data. Numerous other examples of uplifted Pleistocene coastal deposits have recently been described along the Iberian Atlantic margin to the north or south of the study area, with evidence for localized uplift rates of up to 3 mm yr^{-1} (Granja and de

Groot, 1996; Zazo et al., 2003; Carvalho et al., 2006; Alonso and Pagés, 2007; Gracia et al., 2008; Granja et al., 2008).

In an effort to uncover new evidence of Paleolithic coastal occupation, the Estremadura coastline was selected for an intensive archaeological survey in 2005. Because of its proximity to the deep waters of the Nazaré canyon, it was hypothesized that the steep offshore bathymetry would result in limited distances between the modern and Pleistocene shorelines (Dias et al., 2000), and would favor strong upwelling that would make the region favorable for settlement by hunter-gatherer societies (Thomson et al., 2000; Erlandson, 2001). The tectonic setting and long history of human land use in the area complicate Paleolithic archaeological investigations because most Late Pleistocene surfaces are either eroded or deeply buried. A number of Middle Paleolithic sites, many from inland caves, rock shelters, and fluvial settings, record Neanderthal settlement in Estremadura before about 26 ka (Raposo, 2000; Zilhão, 2000). A few of these are coastal sites in central Portugal: Figuera Brava, a cave locality south of Lisbon that dates to around 30 ka (Antunes, 200a,b); Praia do Pedrógão, an as yet undated site north of the Rio Lis (Aubry et al., 2005); and Mira Nascente and Praia Rei Cortiço, which are discussed here and in

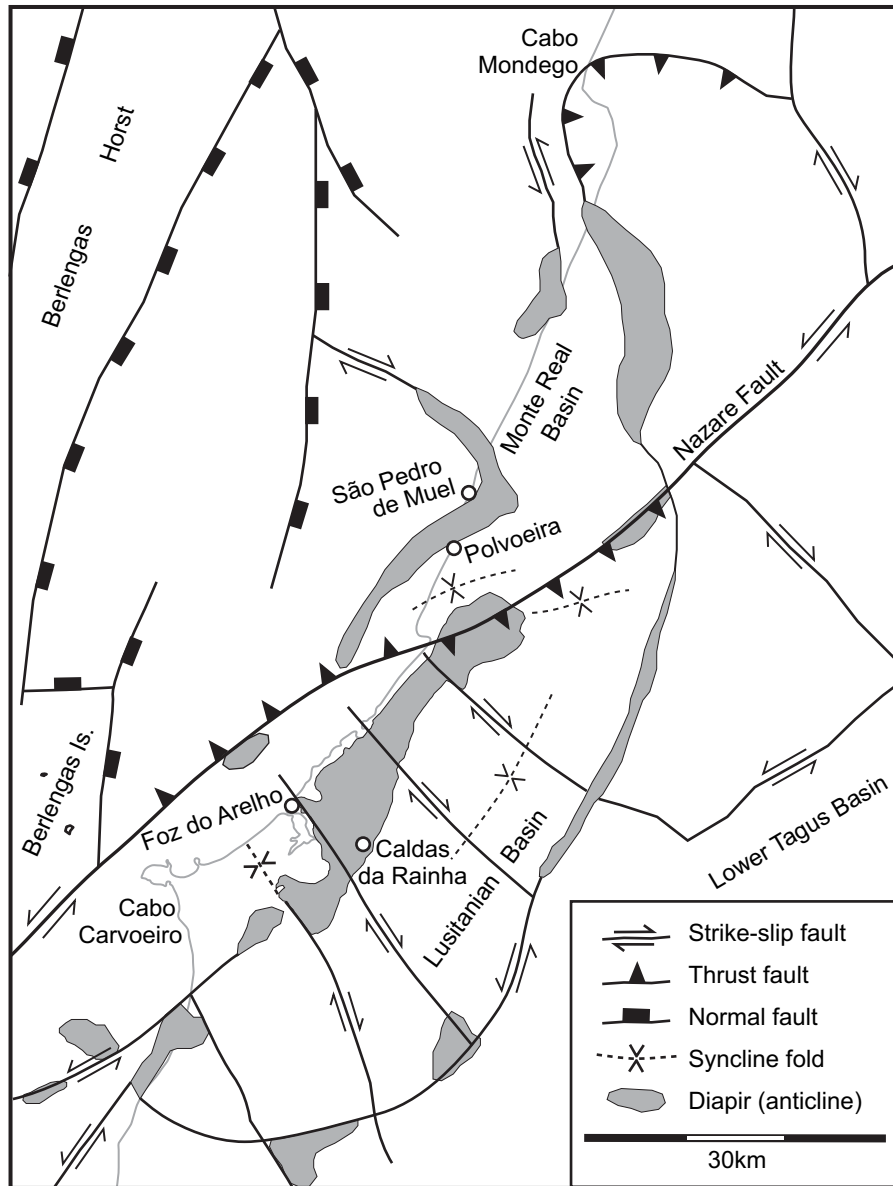


Fig. 2. Major tectonic and structural features in the study area. Major faults adopted from Pinheiro et al. (1996); diapir boundaries from Rasmussen et al. (1998).

Haws et al. (2009). These and a handful of other sites in Portugal yield critical information about Neanderthal and early modern human diet, subsistence, and use of coastal resources (Hockett and Haws, 2005; Finlayson, 2008).

3. Materials and methods

Raised beach sections were measured in the field using conventional stratigraphic methods during 2006–2008. Strata described in this study are allostratigraphic units, defined on the basis of bounding discontinuities marked by paleosols and erosional contacts, with subdivisions based on lithology and sedimentary structures. Elevations were determined to within ± 1 m relative to the mean high tide line (taken as 1.5 m above mean tide, given the tidal range of 2.9 m) using a digital range finder – clinometer. Because of a nearly complete lack of microfossils in these sections, interpretation depends on the presence of sedimentological indicators of depositional environments. These interpretations were aided by geomorphological mapping from

topographic sheets at 1:25,000 and aerial photographs at various scales. Samples were collected from the described sections and from modern depositional environments for detailed particle size analysis using either an ATM LP3 sonic sifter (for sands at 1ϕ intervals) or a Beckman Coulter LS 200 particle counter (for muddy samples). Particle size parameters are reported on the phi scale after the Folk and Ward (1957) graphical method as calculated by the Gradistat program (Blott and Pye, 2001). Magnetic susceptibility was measured at several sites according to the methods described in Ellwood et al. (1995). Detailed results of pollen analysis and archaeological investigations at these sites are described in Haws et al. (2009).

Age determination of the Pleistocene sections was achieved by optically stimulated luminescence (OSL) and AMS radiocarbon methods. OSL samples were collected by inserting opaque PVC tubes into the walls of sampling exposures that were excavated at least 1 m back from the face of the outcrop, avoiding strata with evidence of strong root penetration or pedogenesis. The samples were analyzed at the Luminescence Dating Laboratory, University

Table 1
Sample data for optically stimulated luminescence ages.

Site	Stratigraphic unit	Lab reference	Equivalent dose (Grays) ^a	Ur (ppm) ^b	Th (ppm) ^b	K ₂ O (%) ^b	H ₂ O (%) ^c	Cosmic dose (mGrays/yr) ^d	Total dose (mGrays/yr)	OSL age (yr BP) ^e
São Pedro de Muel	SP2	UIC2069	41.66 ± 0.74	0.5 ± 0.1	1.5 ± 0.1	1.13 ± 0.01	10 ± 3	0.016 ± 0.002	1.17 ± 0.07	35,530 ± 2785
São Pedro de Muel	SP3b	UIC2066	62.52 ± 0.11	0.9 ± 0.1	2.9 ± 0.1	1.63 ± 0.01	10 ± 3	0.016 ± 0.002	1.77 ± 0.08	35,260 ± 2590
São Pedro de Muel	SP3d	UIC2068	56.08 ± 0.50	0.7 ± 0.1	2.2 ± 0.1	1.32 ± 0.01	10 ± 3	0.015 ± 0.001	1.42 ± 0.07	39,450 ± 2980
São Pedro de Muel	SP3f	UIC2067	71.51 ± 0.83	0.8 ± 0.1	2.2 ± 0.1	1.50 ± 0.01	10 ± 3	0.015 ± 0.002	1.54 ± 0.07	46,660 ± 3570
Atlântico Village	AV2	UIC2323	2.30 ± 0.20	0.9 ± 0.1	2.0 ± 0.1	0.91 ± 0.01	10 ± 3	0.16 ± 0.02	1.24 ± 0.06	1850 ± 200
Polvoeira	PV2c	UIC2070	62.69 ± 0.45	0.6 ± 0.1	1.5 ± 0.1	1.77 ± 0.01	10 ± 3	0.015 ± 0.002	1.73 ± 0.08	36,250 ± 2840
Polvoeira	PV4	UIC2071	57.40 ± 1.38	0.7 ± 0.1	1.9 ± 0.1	0.75 ± 0.01	10 ± 3	0.014 ± 0.001	0.92 ± 0.05	62,220 ± 4660
Mira Nascente	MN2	UIC1875	50.10 ± 0.16	0.6 ± 0.1	1.4 ± 0.1	1.36 ± 0.01	10 ± 3	0.028 ± 0.003	1.39 ± 0.07	36,035 ± 2750
Mira Nascente	MN2	UIC1863	61.79 ± 0.15	0.6 ± 0.1	1.2 ± 0.1	1.91 ± 0.02	10 ± 3	0.016 ± 0.002	1.82 ± 0.09	33,905 ± 2690
Mira Nascente	MN3b	UIC1864	50.22 ± 0.05	0.8 ± 0.1	1.5 ± 0.1	1.14 ± 0.01	10 ± 3	0.016 ± 0.002	1.24 ± 0.07	40,450 ± 2980
Mira Nascente	MN3c	UIC1923	47.89 ± 1.00	2.0 ± 0.1	2.7 ± 0.1	1.09 ± 0.01	20 ± 5	0.015 ± 0.002	1.39 ± 0.07	34,300 ± 2630
Mira Nascente	MN4	UIC1868	>140.08 ± 0.08	0.6 ± 0.1	1.2 ± 0.1	1.25 ± 0.01	10 ± 3	0.015 ± 0.002	1.27 ± 0.07	>110,050 ± 8460
Mira Nascente	MN5	UIC2065	139.69 ± 0.68	0.6 ± 0.1	1.8 ± 0.1	0.85 ± 0.01	15 ± 3	0.012 ± 0.001	0.93 ± 0.08	150,920 ± 12,575
Vale Pardo	VP2	UIC2324	86.10 ± 2.31	0.8 ± 0.1	1.8 ± 0.1	1.11 ± 0.01	10 ± 3	0.16 ± 0.02	1.37 ± 0.07	62,855 ± 4590
Vale Pardo	VP3a	UIC2326	42.98 ± 2.10	1.0 ± 0.1	1.9 ± 0.1	1.18 ± 0.01	10 ± 3	0.16 ± 0.02	1.48 ± 0.07	29,100 ± 2415
Praia Rei Cortiço	PC2b	UIC2399	33.58 ± 0.27	1.0 ± 0.1	5.6 ± 0.1	1.70 ± 0.01	10 ± 3	0.16 ± 0.02	2.23 ± 0.12	15,060 ± 980
Praia Rei Cortiço	PC4	UIC2398	71.63 ± 2.58	0.9 ± 0.1	1.4 ± 0.1	0.47 ± 0.01	10 ± 3	0.028 ± 0.003	0.71 ± 0.04	101,010 ± 7870

^a Equivalent dose determined by the multiple aliquot regenerative dose method under green (514 nm) or blue (470 nm) excitation (Jain et al., 2003). Blue emissions are measured with one 3-mm-thick Schott BG-39 and one 3-mm-thick Corning 7-59 glass filters that block >90% luminescence emitted below 390 nm and above 490 nm in front of the photomultiplier tube. The coarse-grained (150–250 μm) quartz fraction is analyzed.

^b U, Th and K₂O determined by ICP-MS at Activation Laboratory Ltd., Ontario.

^c Average water content estimated from particle size characteristics assuming periodic wetting in the vadose zone.

^d Cosmic dose rate component from Prescott and Hutton (1994) based on latitude, longitude, elevation, and burial depth of samples.

^e All errors are at one sigma and ages are calculated from AD 2000. Analyses performed by Luminescence Dating Research Laboratory, Dept. of Earth & Environmental Sciences, University of Illinois, Chicago.

of Illinois, Chicago (Table 1). Equivalent doses were determined by the multiple aliquot regenerative dose method under green (514 nm) or blue (470 nm) excitation (Jain et al., 2003). The coarse-grained (150–250 μm) quartz fraction of each sample was analyzed. The OSL method is well-suited for application in this environment, where sediments are predominantly siliceous and are rapidly buried by littoral processes after long periods of exposure to sunlight on beaches, dunes, tidal flats, or coastal bluffs (Forman et al., 2000). OSL dating has recently been applied with good results to quartz-rich coastal deposits in a similar setting in northwestern Portugal (Thomas et al., 2008).

Where they were encountered, samples of charcoal, peat, and organic sediment were submitted for AMS radiocarbon analysis at Beta Analytic in Miami, Florida or the Center for Applied Isotope

Studies at the University of Georgia. While ages based on charcoal samples are mostly in agreement with the OSL ages, there is a pattern of anomalously young radiocarbon ages obtained from soil organic matter, detrital organic matter in sediment, and thin peat deposits throughout the study area (Table 2). We attribute this to several factors: poor preservation of organic matter in an oxidizing environment, strong podzolization leading to percolation of mobile organic carbon through buried strata, and evidence of root penetration in some muddy and organic-rich horizons. Some of the ambiguity in radiocarbon ages may reflect the residence time and turnover of organic carbon during pedogenesis (Mayer et al., 2008) or limitations on radiocarbon calibration that pose challenges to geological and archaeological investigations of MIS 3 (Blockley et al., 2008; Jöris and Adler, 2008; Weninger and Jöris, 2008; Briant and

Table 2
Sample data for AMS radiocarbon ages.

Site	Stratigraphic unit	Material	Lab reference ^a	Radiocarbon age (¹⁴ C yr BP)	Calibrated Age (cal yr BP) ^b
São Pedro de Muel	SP3a	Organic sediment	Beta 234378	21,640 ± 100	(25,814 ± 492)
São Pedro de Muel	SP3e	Organic sediment	Beta 208226	27,070 ± 230	(31,801 ± 174)
Polvoeira	PV3a	Organic sediment	Beta 234377	13,430 ± 50	(16,382 ± 411)
Mira Nascente	MN3a	Charcoal	Beta 234375	37,540 ± 600	42,175 ± 461
Mira Nascente	MN3a	Soil organic matter	Beta 208223	17,180 ± 80	(20,628 ± 292)
Mira Nascente	MN3b	Charred stump	Beta 208224	21,810 ± 160	(26,110 ± 499)
Mira Nascente	MN3c	Charcoal	Beta 234376	36,720 ± 270	41,717 ± 311
Mira Nascente	MN3c	Charcoal	Beta 208225	36,030 ± 710	40,744 ± 1025
Feliguera Grande	FG2	Charcoal	Beta 208227	2150 ± 40	2180 ± 98
Vale Pardo	VP2	Charcoal	Beta 222201	2610 ± 40	2746 ± 19
Praia Rei Cortiço	PC2a	Peat	Beta 234368	3970 ± 40	4448 ± 56
Praia Rei Cortiço	PC5b	Charcoal	UGAMS 3254	46,850 ± 250	(50,356 ± 1854)
Praia Rei Cortiço	PC5c	Charcoal	UGAMS 3912	49,560 ± 310	(53,781 ± 2055)
Praia Rei Cortiço	PC5c	Charcoal	UGAMS 3255	>49,600	outside range
Praia Rei Cortiço	PC5c	Charcoal	UGAMS 3913	>49,600	outside range

^a Beta: Beta Analytic, Inc., Miami FL. UGAMS: Center for Applied Isotope Studies, University of Georgia, Athens, GA.

^b Calibration curve: CalPal2007_HULU (Weninger and Jöris, 2008). Ages given in parentheses are in disagreement with bracketing OSL ages and are considered anomalous as discussed in the text.

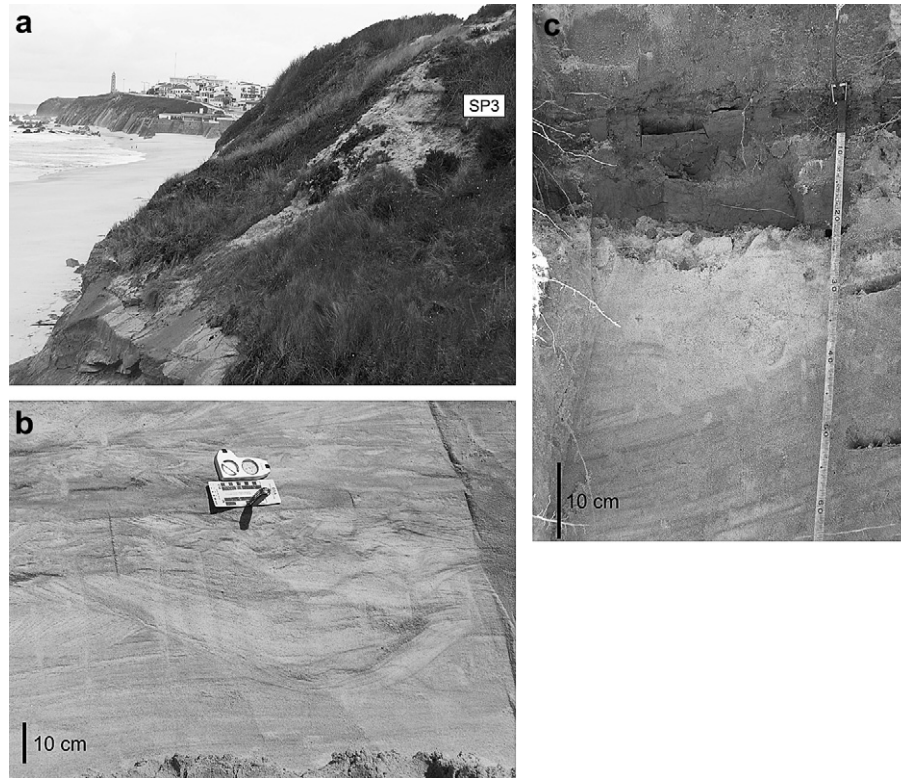


Fig. 3. Photographs from the São Pedro de Muel site. (a) View of coastal bluffs. The described section outcrops in the foreground; two mud beds of unit SP3 are visible. The raised bedrock platform cut across Jurassic limestone beds is visible at the base of the outcrop and beneath lighthouse in background. Modern bedrock platform is exposed in shoaling zone at base of cliffs. (b) Exposure of unit SP2 showing hummocky cross-stratification and ripple lamination typical of inner shoreface deposits. (c) Exposure of SP3c (mud) and SP3d (sand) showing low-angle cross-lamination dipping seaward. Bedding in uppermost 15 cm below mud includes very faint cross-lamination dipping in the opposite direction (obscured by bioturbation).

Bateman, 2009). By contrast, OSL ages obtained in this study are in good agreement with each other and tend to agree with the oldest radiocarbon ages on charcoal samples from the same stratigraphic levels. For convenience, ages discussed in the text are given in calendar years rounded to the nearest thousand years (ka), or to the nearest 0.1 ka for Holocene ages (Tables 1 and 2).

4. Results

4.1. São Pedro de Muel to Polvoeira

The northernmost raised beach in the study area outcrops in the coastal bluffs south of São Pedro de Muel. This locality was described previously by Firtion and Carvalho (1952), who suggested a last glacial age for the raised beach section. The beach deposits are perched atop a roughly horizontal bedrock platform,

10–15 m above mean tide, which is etched across steeply dipping beds of Jurassic limestone on the flanks of a diapiric anticline (Figs. 3 and 4). A narrow modern bedrock platform is exposed immediately offshore at low tide. The village of São Pedro de Muel is located atop the raised platform, which extends at least 2 km inland beneath Holocene aeolian sands. Pleistocene deposits outcrop intermittently in coastal bluffs for several kilometers to the south. To the north, the coastal bluffs and bedrock platform decrease in elevation and are buried beneath a dune field that extends up to 15 km inland from the coast. The coastal dunes in this area were mapped as Holocene in age by França and Zbyszewski (1963), and Clarke and Rendell (2006) have reported Holocene and historical OSL ages for dunes north of São Pedro de Muel. An OSL age of 1.9 ka was obtained for dune sand immediately below a buried A horizon in dune sand at Atlântico Village, 2 km SE of São Pedro de Muel (Table 1).

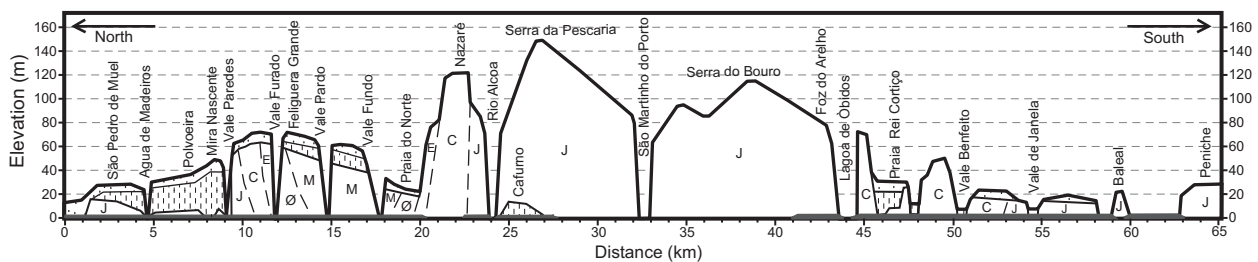


Fig. 4. Cross-section showing elevation and geology of bluffs along the immediate coastline in the study area. Dotted pattern shows Holocene dune sand, dashed pattern shows Pleistocene deposits, dark bar across base of cliffs shows the extent of modern barrier beach. Bedrock symbols: M – Miocene, Ø – Oligocene, E – Eocene, C – Cretaceous, J – Jurassic. Place names are given for comparison with Fig. 1. Data derived from field notes, topographic sheets (1:25,000), and geologic boundaries of França and Zbyszewski (1963).

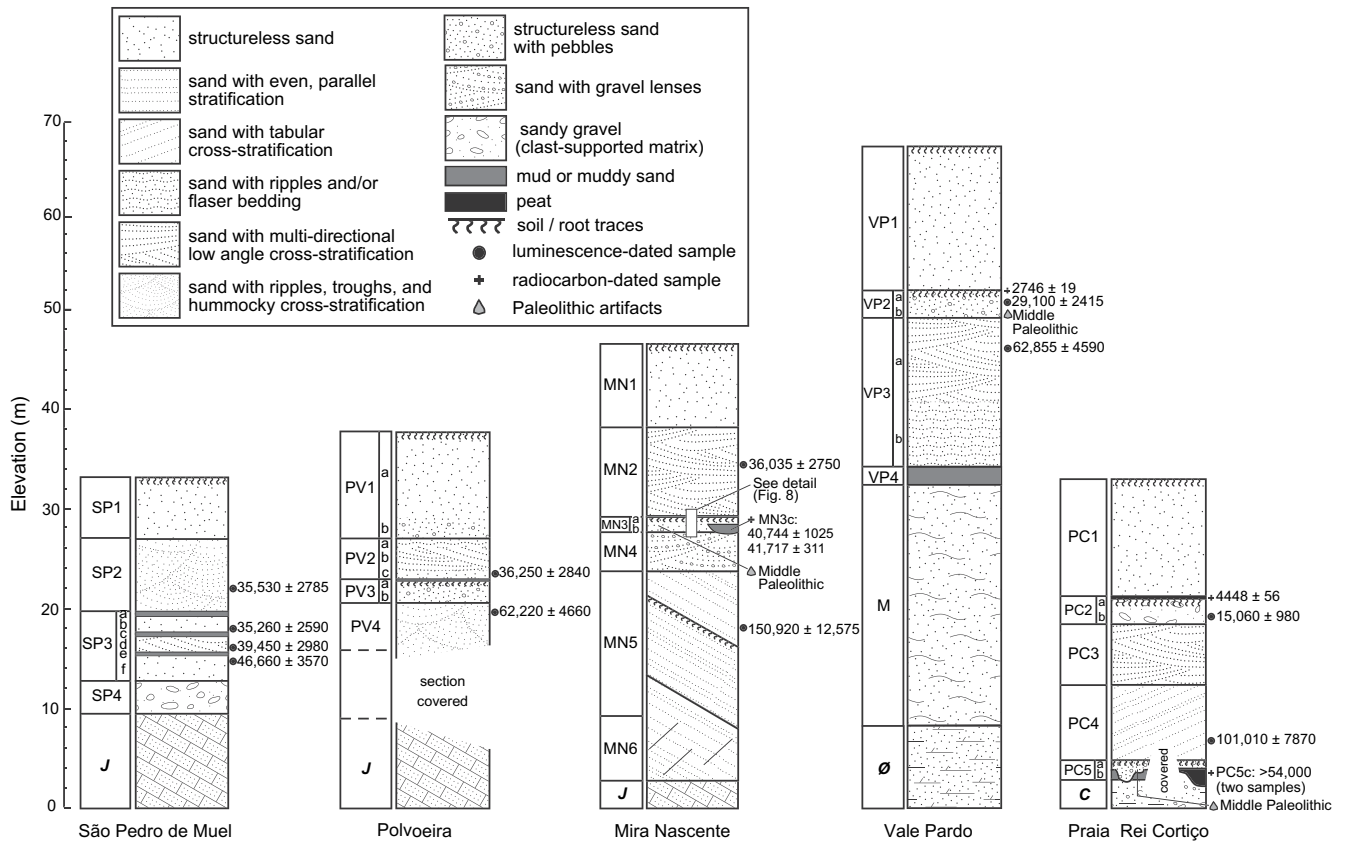


Fig. 5. stratigraphic data for coastal bluff sections with age control.

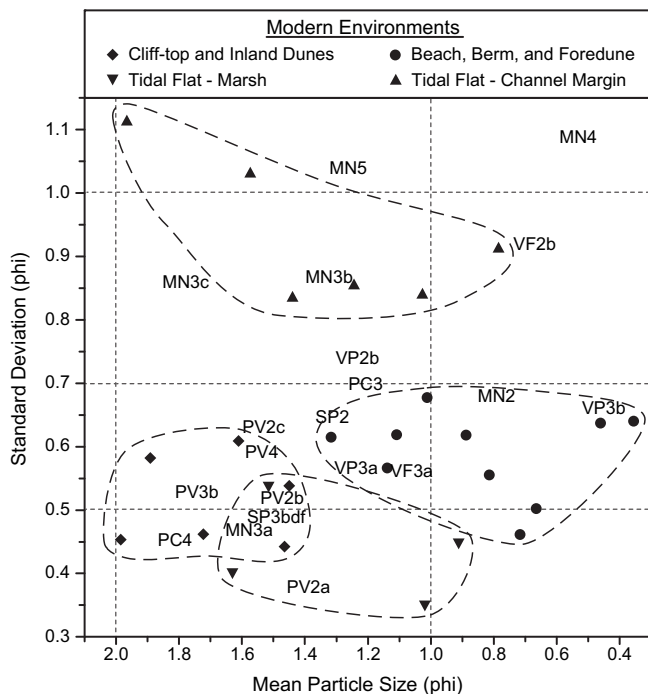


Fig. 6. Particle size comparison of Pleistocene samples from coastal bluffs with samples from modern depositional environments in the vicinity of Nazaré. Bluff samples are labeled with stratigraphic unit ID (see Fig. 5). Dashed lines delineate plot space occupied by modern dune, beach, tidal flat, and tidal channel margin deposits.

The raised beach at São Pedro de Muel includes a clast-supported gravel lag resting on the raised bedrock platform, overlain by alternating beds of sand and mud, capped by aeolian sands at the surface (Fig. 5). The gravel of SP4 is undated but likely represents beach deposits related to erosion of the bedrock platform. OSL ages assign the sand/mud complex of SP3–2 to the middle of MIS 3, roughly 47–35 ka. The thin mud layers of SP3 (a,c,e) trace laterally for at least 200 m in bluff exposures. SP3 muds contain laminations of fine sand, faint mottling by root traces in the sand beds beneath, and flame structures into the sand beds above. SP3 sand layers are massive or contain faint low-angle cross-laminations dipping both landward and seaward in a chevron pattern. Unit SP3 bears some resemblance to “wet aeolian” deposits described along the north-western Portuguese margin by Granja et al. (2008) and for the Bay of Cadiz by Zazo et al. (2008). However, particle size parameters of these sands resemble samples collected from modern tidal flats in the study area (Fig. 6). We interpret SP3 as an intertidal complex on the basis of the sedimentological indicators (described above), the presence of coastal pollen assemblages and plant remains (below), and the overlying beach/shoreface unit (SP2, below) that strongly suggests a transgressive coastal sequence. It was likely deposited in a low-energy environment, possibly a back-barrier flat including overwash and intertidal pool facies. The lack of thick slackwater deposits or marine microfossils argues against an origin in a large, isolated lagoon or estuary.

The mud beds within SP3 (a,c,e) contain some limited paleo-environmental information in the form of pollen and plant remains. Recent pollen analysis of these mud beds (Haws et al., 2009) found a very low abundance of Poaceae, *Picea*, *Tilia*, *Acer*, *Plantago*, *Pinus*, and other unidentifiable grains. Firtion and Carvalho (1952) reported pollen results from three mud layers in a coastal bluff at

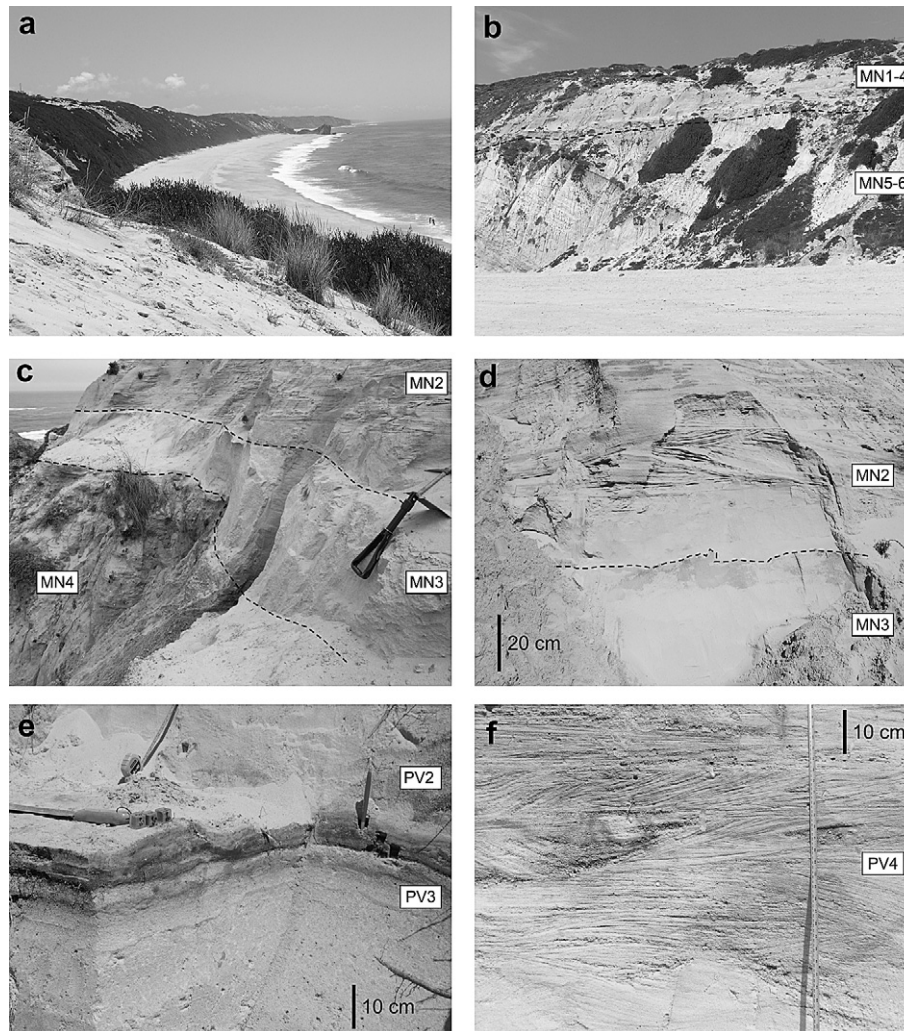


Fig. 7. Photographs from the Mira Nascente and Polvoeira sites. (a) View of coastal bluffs between Polvoeira site (sand in foreground) and Mira Nascente site (adjacent to bedrock spur in background). Bedrock spur in surf zone at Mira Nascente runs parallel to Vale Paredes. (b) View of Mira Nascente bluff from beach level. Units MN1–4, flat lying, exposed in upper bluff; units MN5–6, dipping south, exposed in lower bluff. (c) Bluff view at Mira Nascente showing upper beach complex (MN2), white sand with Middle Paleolithic artifacts (MN3), and lower pebbly beach/colluvium (MN4). (d) Detail of MN2–3 contact showing low-angle multi-directional cross-stratification in MN2, massive sand at base of MN2, and truncated mud deposit at top of MN3. (e) Detail of unit PV3, showing rippled mud bed with faint root or burrow traces and clay lamellae in underlying massive sand. (f) Detail of unit PV4 showing low-angle cross bedding, hummocky cross-stratification, and lenses of coarse sand with pebbles.

São Pedro de Muel, presumably the same beds described here. They also commented on the low abundance and poor preservation of pollen in the sediments, finding *Pinus pinaster* with some *Betula*, *Corylus*, *Rhus*, *Ericaceae* (*Rhododendron*), and *Compositae* (*Carduus*). In addition to pollen, Firtion and Carvalho (1952) reported finding debris of *Phragmites* and roots of *Cyperaceae*, reeds and sedges that are common to estuaries and back-barrier lagoons. *Phragmites* is associated with brackish water, tolerating salinities in the range of 2–22 g l⁻¹ (Rodwell, 1995), supporting the interpretation of an intertidal depositional setting for these muds.

Above the uppermost mud of SP3 rests a 7-m-thick unit of partly indurated sand and pebbly sand with an OSL age of 36 ka (SP2). Structures in this deposit include thin planar cross-beds dipping gently oceanward, ripple-laminated beds with coarse sand and pebbles, and hummocky cross-stratification. The hummocky strata include concavo-convex laminae that converge upwards over hummocks and diverge downwards to fill troughs that truncate the underlying strata (Fig. 3). These structures indicate deposition on the shoreface, below mean low tide but above the storm wave base (Myrow and Southard, 1991). The deposits of SP2 are likely composed of reworked sand from the SP3 complex, which may

explain the virtually identical OSL age of sand recovered from the upper part of SP3 and the lower part of SP2. Saltation of coarse sand grains in the shoreface water column may have prevented complete resetting of the luminescence signal in SP2 as discussed by Forman (1999). The entire sand–mud complex of SP3–2 yields OSL ages from 47 to 35 ka, values that mostly fall in stratigraphic sequence and compare favorably with ages from the Mira Nascente and Polvoeira sites described below. However, radiocarbon analysis of detrital organic matter in the mud layers of SP3 consistently underestimated their ages relative to the OSL ages of bracketing sand layers (Tables 1 and 2). We consider these ages to be anomalous as discussed above.

4.2. Polvoeira to Vale Paredes

The coastal section from Polvoeira south to Mira Nascente is marked by increasing relief of the coastal bluffs and increasing thickness of the preserved Pleistocene section (Fig. 4). The uplifted bedrock platform continues south from São Pedro de Muel to Polvoeira, while the platform at modern sea level widens and diverges from the beach at Polvoeira, following the southern limit of the São

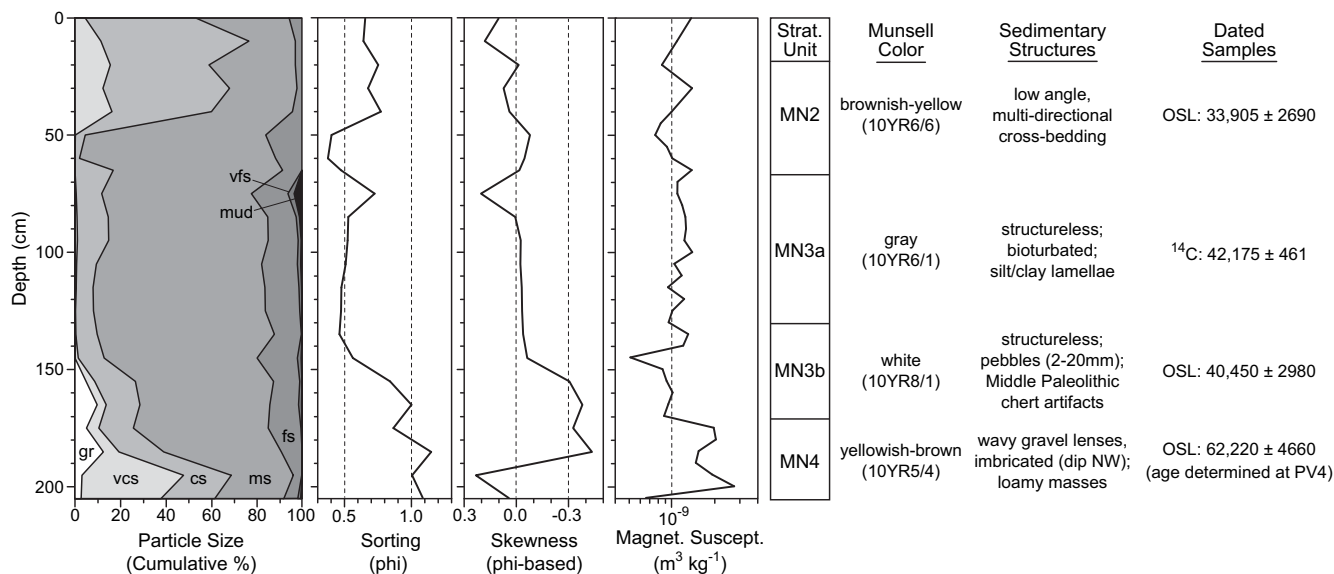


Fig. 8. Detailed particle size data, magnetic susceptibility measurements, sedimentological description, and sample ages for the white sand layer (MN3) at Mira Nascente site. Photo of the sampled section is shown in Fig. 7b.

Pedro de Muel diapir (Fig. 2). An isolated spur of Jurassic bedrock in the surf zone at Mira Nascente (Fig. 7) is aligned perpendicular to the coast, parallel to a deep, straight valley that heads about 3 km inland (Vale Paredes, likely structurally controlled). The Pleistocene section at Mira Nascente demonstrates evidence of neotectonic deformation associated with these structural features. The lowest exposed unit (MN6) contains orthogonal fractures that display up to 20 cm of displacement, and the lower sand beds (MN5–6) dip towards Vale Paredes at roughly 30° south. The overlying strata (MN1–4) are roughly horizontal and rest unconformably on top of the dipping beds.

The upper units at Mira Nascente and Polvoeira (MN1–4, PV1–4) can be traced laterally along exposures in 1 km of coastal bluffs between the two sites. These beds have a gentle northward dip so that the elevation of each unit is about 10 m lower at Polvoeira than at Mira Nascente (Fig. 5). They include a lower beach unit (MN4, PV4), a tidal flat (MN3, PV3), an upper beach/tidal complex (MN2, PV2), and Holocene dune sand (MN1, PV1). At Polvoeira the lower beach deposit (PV4) is dated to around 62 ka (MIS 4–3 transition). It includes medium to coarse sand and pebbles, with ripple-laminated beds and hummocky cross-stratification suggestive of deposition in the upper shoreface (Fig. 7). At Mira Nascente, the deposit (MN4) is a pebbly beach deposit with gravelly lenses that are imbricated with a seaward dip. MN4 also has some characteristics of colluvial deposition, including irregular-shaped loamy masses with matrix-supported pebbles. Because the entire deposit can be traced laterally between the two sites, we consider 62 ka to be the likely age of both PV4 and MN4. The much older and uncertain age for MN4 (>110 ka, Table 1) is likely the result of colluvium incorporated into the beach by wave action undercutting of the bluffs, without allowing time for complete resetting of the luminescence signal.

The most prominent stratigraphic feature in this coastal section is a 1–2 m thick layer of massive white sand (PV3, MN3) that contains useful information in the form of weathering features, paleotopography, pollen, and a Middle Paleolithic archaeological site (Figs. 7 and 8). At Polvoeira, the white sand is capped by a 5–10 cm thick bed of muddy sand (PV3a) with ripple laminations and a hummocky surface topography (Fig. 7). Beneath the mud is gray sand with faint mottling due to bioturbation in the upper 20–30 cm, grading downward into massive white medium sand with well rounded pebbles and clay lamellae (PV3b). The mud bed is

fully preserved only at Polvoeira, but the mottled gray sand and massive pebbly white sand trace laterally to Mira Nascente (MN3ab) where the mud was presumably eroded during the deposition of unit MN2. Magnetic susceptibility measurements on the detailed section between MN2–3–4 show very low values around 10^{-8} – 10^{-9} m³ kg⁻¹, with a slight increase in the suspected colluvial masses of unit MN4 (Fig. 8). These values are consistent with a coastal or marine origin for the MN2–3 sands, with virtually no evidence of pedogenic iron present (Ellwood et al., 2000; Yim et al., 2004). Based on the available evidence (wave-rippled mud, bioturbation, low magnetic susceptibility, and particle size parameters) we identify PV3/MN3 as a tidal flat with channel deposits at depth capped by a muddy marsh surface.

At Mira Nascente, archaeological excavations in unit MN3b recovered an assemblage of points, flakes, and cores made of reddish-brown chert. Several of these are Levallois type, a Mousterian technique that is diagnostic of Neanderthal populations during the Middle Paleolithic (Haws et al., 2009). Use-wear analysis on the flakes is consistent with cutting soft bone and tissue, possibly for butchering of fish. Additional Middle Paleolithic artifacts were recovered 200 m to the north, from the white sand bed exposed in the bluffs between Mira Nascente and Polvoeira. About 50 m south of the archaeological site at Mira Nascente, unit MN3a merges with the margin of a channel fill deposit of organic muddy sand (MN3c). Pollen recovered from MN3c is dominated by Ericaceae (*Calluna* or *Erica*), Poaceae, and Cistaceae (*Tuberaria guttata*), suggesting a dry coastal heath community (Haws et al., 2009).

The gently undulating topography of PV3/MN3 between Mira Nascente and Polvoeira suggests a broad tidal flat bordering a channel possibly connected to the Vale Paredes drainage. A suite of OSL and AMS radiocarbon ages on charcoal firmly establish the age of this deposit at 40–42 ka, in good agreement with the Late Middle Paleolithic cultural attribution (Fig. 8). A notable exception is one OSL age on sand within the paleochannel (MN3c) which corresponds with the age of the overlying beach sand (MN2), while radiocarbon ages from MN3c agree with the other ages from units MN3a and MN3b. This evidence suggests that the paleochannel accumulated organic matter during the deposition of MN3a (42 ka), and was backfilled with sand during the relative sea level rise represented by MN2 (34–36 ka).

The PV3/MN3 complex is overlain by a younger beach complex with ages between 34 and 36 ka. At Mira Nascente (MN2) this unit contains coarse sand with low-angle cross-laminations dipping both landward and seaward, interpreted as beach run-up and berm overwash deposits (Figs. 7 and 8). A structureless sand bed at the base of MN2 truncates the top of MN3, suggesting encroachment of foredunes or overwash deposits at the beginning of the transgressive sequence. At Polvoeira the upper beach complex includes a series of ripple-laminated and tabular low-angle cross-laminated sand beds (PV2a,b,c). Units MN2, PV2, and SP2 contain the youngest raised beach deposits in the study area. They appear to record the final relative sea level rise during MIS 3 before sea level dropped to the low levels of the glacial maximum during MIS 2. The top of the beach deposits are truncated by massive pebbly sand that grades upwards into Holocene dune sand (PV1a,b). The pebbly deposits are interpreted as colluvium deposited on the coastal bluffs during MIS 2, similar to the colluvial deposits described below for the bluffs at Vale Pardo.

4.3. Vale Paredes to Nazaré

Immediately south of Vale Paredes the coastal bluffs are composed of Mesozoic and Cenozoic bedrock cliffs which reach maximum elevations of more than 80 m and progressively descend to less than 20 m north of Nazaré (Fig. 4). The bedrock structure of this coastal section forms an inland-striking syncline that has been uplifted by some combination of compression along the Nazaré fault and salt tectonics of the São Pedro de Muel diapir. Raised Pleistocene beach deposits are exposed between the Paleozoic bedrock and the Holocene dunes that extend inland from the cliff-tops (Fig. 9). Exposures of the Pleistocene section were described at the rapidly eroding headlands south of Vale Pardo (Fig. 5) and in other exposures between Vale Furado and Vale Fundo. The Pleistocene section thickens from a few meters at Feliguera Grande to more than 10 m at Vale Fundo; south of Vale Fundo the Pleistocene section is either absent or entirely buried beneath aeolian sands.

A prominent paleosol is exposed in the coastal bluffs at the base of the Holocene dune sand, at elevations between 50 and 65 m. It is characterized by a dark Ab horizon with abundant charcoal over well-developed Eb and Bhb horizons suggesting a prolonged period of podzolization (Table 3; Fig. 9). The upper parts of this paleosol are formed in massive pebbly sand that we interpret as colluvium (VP2), while the Bhb horizon in places extends downwards into the underlying beach sands (VP3). The buried A horizon in pebbly sand was identified at the base of the aeolian sands in auger samples and roadcuts up to 2 km inland from Vale Fundo (Fig. 10). Charcoal samples from Ab horizons at Vale Pardo and Feliguera Grande yield ages of 2.2 ka and 2.7 ka, in rough agreement with the OSL age of dune sand beneath an Ab horizon near São Pedro de Muel (AV2, Table 1). An OSL age of 29 ka was obtained on massive medium sand in the Eb horizon at Vale Pardo, suggesting a long period of pedogenesis following deposition of the colluvium. This appears to be the same strongly podzolized soil profile used by França and Zbyszewski (1963) to distinguish Pleistocene aeolian/alluvial deposits from Holocene deposits throughout the study area.

The archaeological survey recovered a low-density scatter of artifacts from the colluvial unit at Vale Pardo (VP2). A single flake with a “Chapeau de Gendarme” platform, indicative of Neanderthal populations in the Middle Paleolithic, was identified during surface collection. No intact cultural features or other diagnostic artifacts were located during testing. Additional artifacts, likely Upper Paleolithic, were recovered as surface finds in areas where the pebbly colluvium outcrops in the bluffs around Vale Fundo. Given the late survival of Neanderthals in Iberia, Middle and Upper

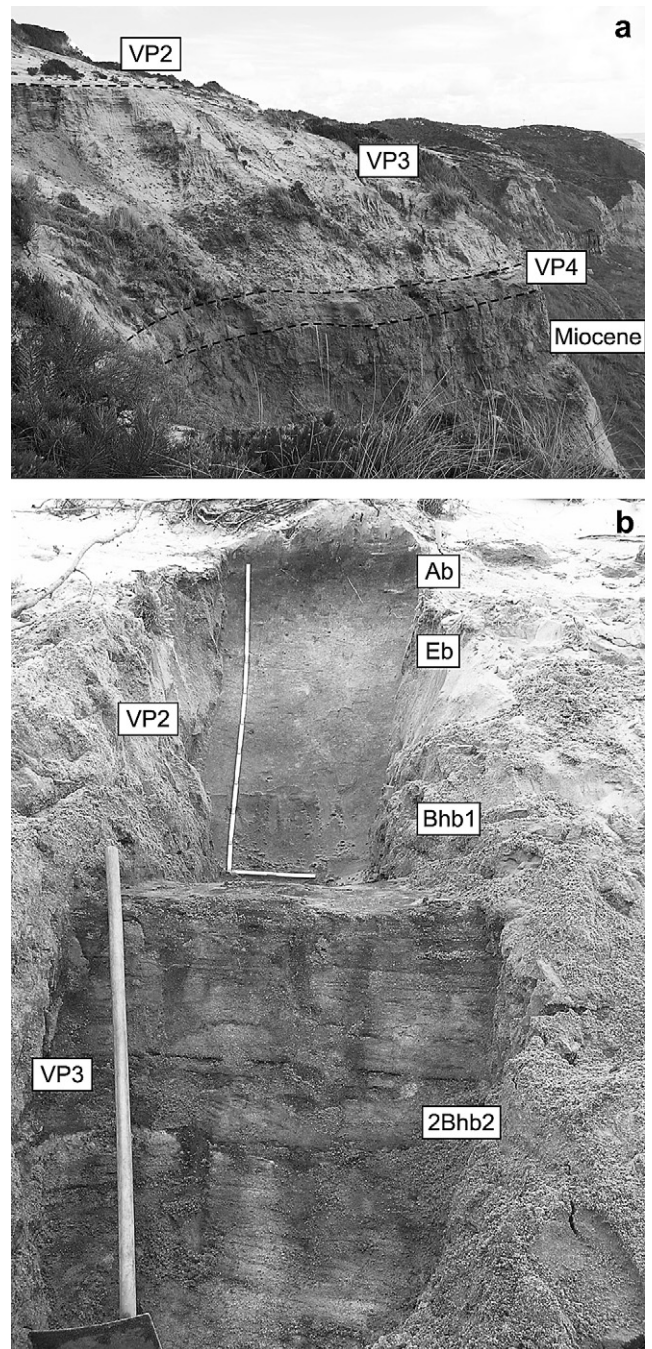


Fig. 9. Photographs from the Vale Pardo site. (a) View of the coastal bluff at Vale Pardo showing Pleistocene colluvial unit (VP2), raised beach (VP3), and mud (VP4) atop Miocene cliffs. (b) Prominent paleosol at Vale Pardo formed in Pleistocene colluvium (VP2) and beach (VP3) deposits. Soil profile description for this exposure is in Table 3.

Paleolithic artifacts are consistent with the deposition of the colluvial unit around 29 ka, followed by a long period of exposure at the surface before being buried by the Holocene dunes.

Below the colluvial unit is a raised beach complex with an OSL age virtually identical to the lower beach deposits at Polvoeira (63 ka). The top of this unit generally includes moderately well-sorted medium to coarse sand with low-angle cross-beds dipping landward and seaward (VP3a). The lower sections include moderately sorted pebbly medium and coarse sand that is ripple-laminated or cross-laminated, with localized loamy masses and flaser bedding (VP3b). This beach/shoreface complex overlies a blue-gray

Table 3
Paleosol characteristics at Vale Pardo bluff site.

Strat. unit	Horizon	Depth (cm)	Lower boundary	Munsell color	Texture class	Rupture resistance	Other features	Sedimentary structures
VP2a	Ab	0–35	gradual, smooth	v. dk. gray (10YR3/1)	medium sand	soft	charcoal, krotovena	massive
VP2b	Eb	35–95	gradual, smooth	lt. brownish-gray (10YR6/2)	slightly gravelly medium sand	soft	pebbles (2–10 mm), root casts	massive
VP2b	Bhb1	95–135	abrupt, smooth	brown (10YR4/4)	gravelly medium sand	soft	pebbles and gravels (2–30 mm)	massive
VP3a	2Bhb2	135–270	clear, irregular	yellowish brown (10YR5/6) and v. dk. brown (7.5YR2.5/3)	medium sand	moderately to very hard	dark masses in vertical streaks and along bedding planes	even parallel lamination, cross-lamination dipping both landward and seaward
VP3a	2C1	270–380	gradual, smooth	v. pale brown (10YR7/4)	slightly gravelly medium sand	soft to slightly hard	pebbles (2–5 mm)	even parallel lamination, cross-lamination dipping seaward, pebbly lenses
VP3b	2C2	380–500	n/a	v. pale brown (10YR7/3) and reddish-yellow (7.5YR6/8)	slightly gravelly coarse loamy sand	soft	pebbles (2–5 mm)	even parallel lamination, ripple lamination, pebbly lenses, flaser bedding

pebbly mud (VP4) that marks the base of the Pleistocene section in coastal bluffs and roadcut exposures between Vale Furado and Vale Fundo. Moderately well-sorted coarse sands in the auger test holes suggest that another raised beach or fluvial deposit may be preserved beneath the colluvial deposits at 70–80 m elevation (Fig. 10).

4.4. Nazaré to Foz do Arelho

The Caldas da Rainha diapir is in closest proximity to the ocean along the coastal section south of Nazaré. Steeply dipping Mesozoic beds on the western flank of the diapir form a narrow coastal ridge up to 160 m high between Nazaré and Foz do Arelho. Strike-slip faults trending NW–SE through the diapir intersect the coastal ridge at Nazaré, São Martinho do Porto, and Foz do Arelho, forming narrow gaps where coastal-draining rivers reach the ocean (Fig. 2). A fluvial terrace at 20–30 m elevation around the margin of the Nazaré and São Martinho do Porto lagoons marks the maximum

Pleistocene fill of the diapiric valley, which is at least 30 m thick in the vicinity of Nazaré (Henriques and Dinis, 2006).

Due to the high cliffs plunging steeply to the sea, there is only limited beach and dune formation along this coastal section and virtually no Pleistocene deposits are preserved. The lone exception is an elongated terrace of well-sorted medium sand attached to the coastal bluff south of Nazaré, near the village of Cafurno (Fig. 11). The terrace is undated by absolute methods but was mapped as a Pleistocene feature by França and Zbyszewski (1963) and demonstrates a podzolized soil profile similar to that of the colluvial units at Vale Pardo (Table 3). The terrace surface resembles an attached beach barrier backed by climbing dunes; it slopes irregularly downhill and flattens at an elevation of 20–30 m, where it is truncated by a scarp at the edge of the Nazaré lagoon. The Cafurno terrace tread corresponds roughly with the elevation of a Pleistocene fill terrace on the landward side of the coastal bluffs, suggesting that both may have been graded to the same former base level.

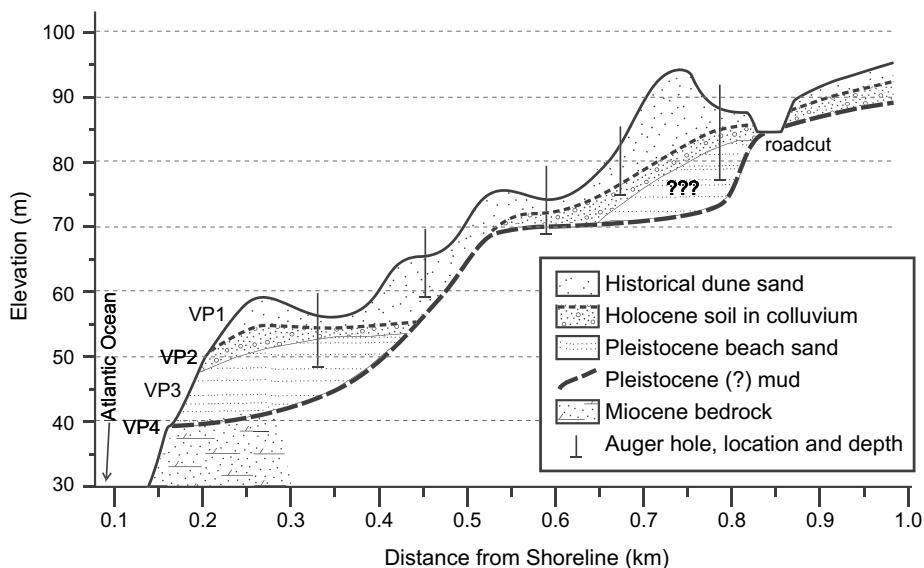


Fig. 10. Cross-section from the top of the coastal bluff near Vale Pardo to a roadcut exposure about 1 km inland. Subsurface data inferred from bluff and roadcut exposures and 4 bucket auger tests.

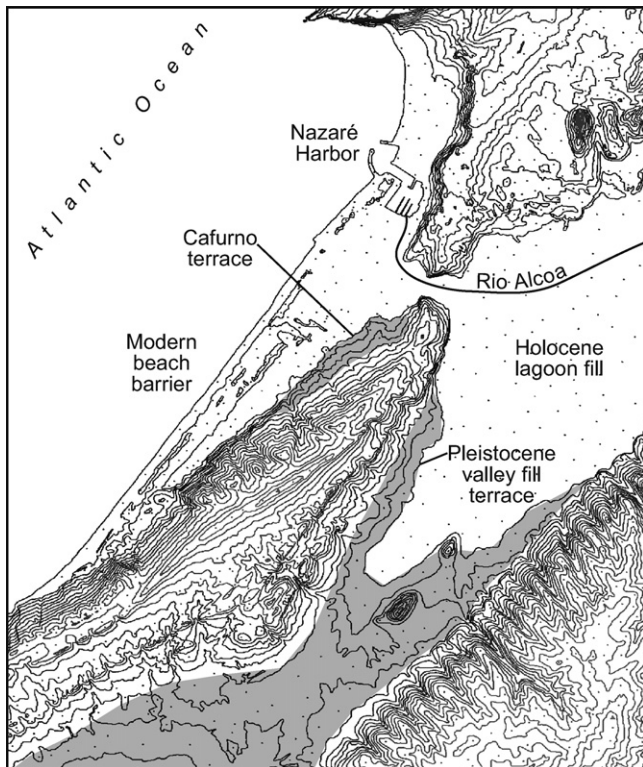


Fig. 11. Topographic map of the coastline south of Nazaré harbor. Shaded areas mark the coastal terrace near Cafurno and the inland diapiric valley fill terrace, both mapped as Pleistocene by França and Zbyszewski (1963). Contour interval 10 m.

4.5. Foz do Arelho to Peniche

South of the Óbidos lagoon, Cretaceous sandstones and conglomerates outcrop in steep coastal cliffs up to 70 m high. In the vicinity of Praia Rei Cortiço, a thick Pleistocene section is preserved in a paleovalley inset into the bedrock and exposed in coastal bluffs (Figs. 4 and 12). The paleovalley drained to the north as a former arm of the Óbidos lagoon system. Lying in a shallow depression at the bottom of the paleovalley is a 2-m-thick peat bed (PC5c) which has been intermittently exposed at the base of the bluff following coastal storms (Fig. 12). The deposit contains abundant charcoal and macrofossils of charred *Pinus* bark and roots. Initial pollen analyses from this unit suggest a seasonally wet/dry *Ericaceae* bog surrounded by mixed coniferous/deciduous forest. Two radiocarbon samples from this unit yielded infinite ages, with a third at the limit for radiocarbon dating (Table 2).

Most of the Pleistocene section at Praia Rei Cortiço is a sequence of aeolian, littoral, and fluvial sand and gravel (Fig. 5). Immediately above PC5 is a cross-bedded aeolian sand (PC4) that fills the entire width of the paleovalley and has an OSL age of 101 ka. This unit includes a 5–6 m thick tabular foreset bed, with laminae dipping at about 30° southeast recording aeolian sand invasion of the paleovalley during MIS 5. The overlying unit (PC3) is a beach deposit of medium to coarse sand with laterally extensive planar beds that dip gently seaward, localized ripple lamination, and gravelly lenses with imbricated pebbles dipping seaward. At the same elevation as the base of PC3, a wave-cut notch and bench are eroded into the Cretaceous bedrock along the southern wall of the paleovalley (Fig. 12). These provide supporting evidence for the interpretation of PC3 as a littoral deposit. Unit PC3 is undated but given the bounding OSL ages it may correlate with one of the MIS 3 beach complexes described along the coast north of Nazaré. PC3 grades

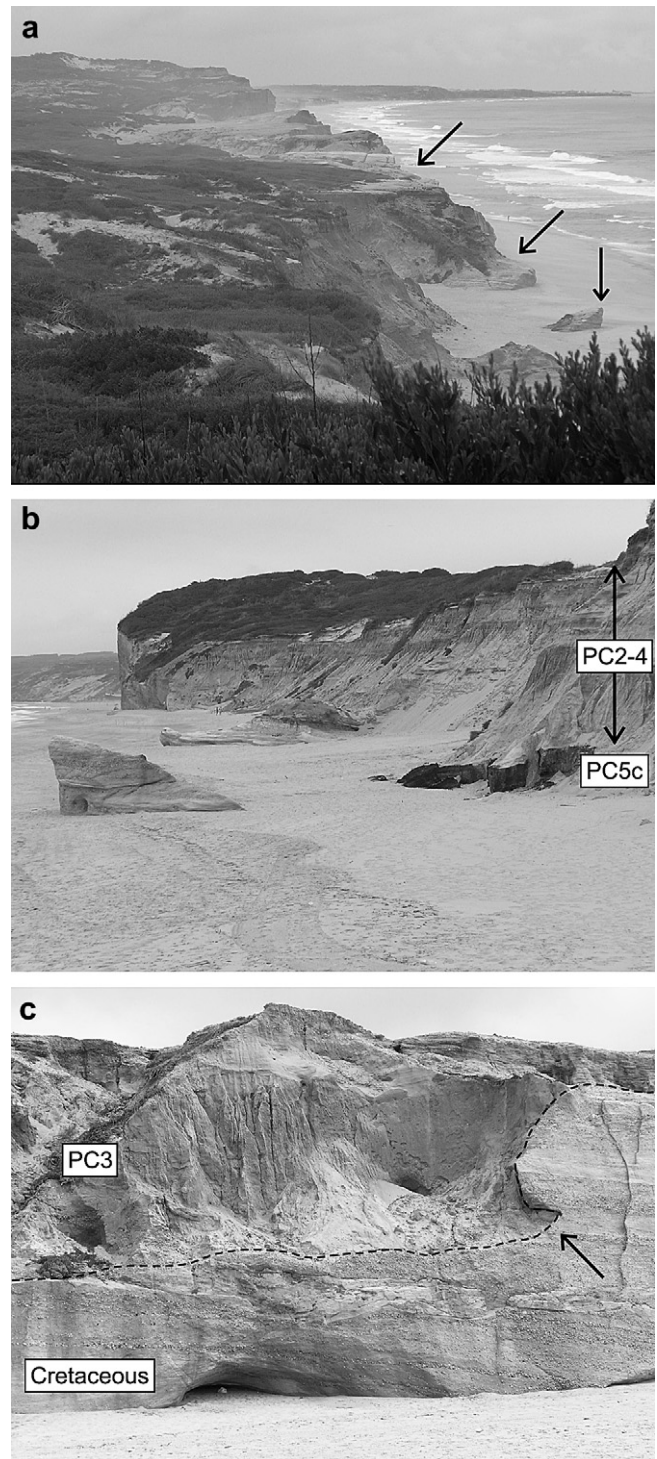


Fig. 12. Photographs from the Praia Rei Cortiço site. (a) Bluff-top view of the paleovalley south of the Óbidos lagoon. Arrows show light-colored Cretaceous bedrock outcrops along margins of paleovalley. Darker-colored sediments exposed in bluff are Pleistocene valley fill units (PC2–5). (b) View to north of Praia Rei Cortiço site from beach level. Pleistocene bog deposit (PC5c) visible in foreground beneath aeolian, littoral, and fluvial deposits (PC2–4). Archaeological site (PC5a,b) is at base of bluffs in the distance. (c) Bench and wave-cut notch in Cretaceous bedrock at southern margin of paleovalley. The flat bedrock bench is at the same elevation as the bottom of unit PC3.

upwards into a very gravelly fluvial sand (PC2) with strong imbrication (gravels dipping upvalley) and well-defined paleochannel margins, with an OSL age dating to late MIS2 (15 ka). A 20 cm thick peat deposit (PC2a) atop the fluvial bed yielded an AMS

radiocarbon age of 4.4 ka, suggesting a rising water table in the valley at the end of the Holocene transgression. The aeolian sand (PC1) at the top of the unit is Late Holocene or historical in age, similar to the section near Vale Pardo.

A Middle Paleolithic archaeological site was uncovered in the base of the bluff at Praia Rei Cortiço, about 200 m north of the lower peat bed (PC5c) but separated from it by recent colluvium (Fig. 5). The site is associated with muddy tidal flat deposits similar to those found at Polvoeira and Mira Nascente. Unit PC5a includes ripple-laminated muddy sand bed atop a massive white pebbly sand bed with faint root traces and clay lamellae extending downwards 20–30 cm from the mud. Middle Paleolithic artifacts were recovered from the underlying silty layer with abundant charcoal (PC5b). The artifact assemblage includes a few burned chert flakes displaying fractures and potlids, and Levallois flakes that confirm Neanderthal occupation at the site during MIS 5 or earlier (Haws et al., 2009). Charcoal in association with the artifacts yielded a (barely) finite radiocarbon age, but it is likely much older if the OSL age of the overlying aeolian sand is accepted. The site is located on the margin of a paleochannel incised into unit PC5b that probably traces laterally to the PC5c bog deposit.

South of Praia Rei Cortiço, the Cretaceous and Jurassic beds have a northward dip and form a nearly level plateau at an elevation of 40–50 m (Fig. 4). The coastal bluffs form near-vertical cliffs topped by a gravel lag that is locally covered by aeolian sand. Several valleys cut into the coastal bluffs in this section contain remnants of organic-rich Pleistocene fluvial or coastal fills, which are limited to the lowermost reaches of the valleys below about 20 m elevation. Diniz (2003) reported pollen assemblages from 4 of these organic valley fills between Figuera da Foz and Peniche, with radiocarbon dates between 35 and 45 ka. These included arboreal *Pinus*, *Quercus*, and *Betula*, with abundant heath (*Ericaceae*) and Mediterranean taxa (*Olea*, *Cistaceae*, *Poaceae*). The full pollen assemblages are as yet unpublished, and the age of these deposits should be regarded with caution in light of the problems with anomalous radiocarbon ages dating to MIS 3. If they correlate with the organic valley fill deposit at Praia Rei Cortiço (PC5c), these fills may in fact be much older.

5. Discussion

5.1. Facies interpretations of the Pleistocene coastal deposits

To use the Estremadura deposits for sea level or tectonic reconstruction, and for correlation with other paleoenvironmental records, it is essential to establish their position relative to sea level at the time they were deposited. High-resolution relative sea level reconstructions usually rely on fossil assemblages as indicators of intertidal, pelagic, or deep ocean environments (Haslett, 2000). However, fossil evidence in the Estremadura raised beach sections is mostly limited to terrestrial pollen and faint root or burrow traces. Poor preservation of marine fossils along this coast is the result of siliclastic mineralogy, strongly acidic soil and vadose water, and steep coastal topography/bathymetry. Large portions of the Portuguese and Spanish Atlantic coasts are fringed by bedrock platforms with sandy Pleistocene sedimentary cover; the relative sterility of these deposits is recognized as a challenge to paleoenvironmental and archaeological reconstructions (Ferreira, 1991; Zazo et al., 1999; Meireles and Texier, 2000; Alonso and Pagés, 2007; Bicho and Haws, 2008). With few biostratigraphic indicators to rely on, these studies typically cite sedimentological, morphological, and geochemical indicators to assign a marine or terrestrial origin to Pleistocene sediments on coastal platforms. Araujo et al. (2003) caution against broad regional generalizations regarding coastal sedimentology, given the tectonic complexity and uncertain sea level history of the coast.

Despite these limitations, several independent observations lead us to conclude that most of the Pleistocene units on the Estremadura bluffs are coastal (intertidal or nearshore subtidal) in origin. Foremost is the prevalence of sedimentary structures that are common in littoral deposits, some of which are considered to be diagnostic of tidal flow or waves (Table 4). These observations are supported by similarities between particle size parameters of the Pleistocene units and modern beach and tidal flat deposits (Fig. 6), and their mineralogical maturity and very low magnetic susceptibility. The fact that these are nearly flat-lying strata etched into

Table 4
Sedimentary facies associations in bluff exposures.

Facies	Particle size	Sedimentary structures	Elevation when deposited	Stratigraphic units (this study)
Aeolian	medium to fine sand; moderately well to well-sorted; symmetrical to coarse skewed	tabular beds with faint low-angle (<12°, ramp) and high-angle (~30°, slipface) cross-lamination	>2 m	SP1, PV1a, MN1, FG1, VP1, VF1, PC1, PC4
Beach and Berm	medium to coarse sand; moderately well sorted; symmetrical to fine skewed	even parallel lamination, cross-lamination dipping seaward (beach) and landward (berm); localized ripple lamination and flaser bedding	5 ± 5 m	MN2, PV2b, FG3, VP3ab, VF3ab, PC3
Shoreface	medium sand; moderately well to well sorted; symmetrical to coarse skewed	parallel lamination dipping gently seaward; symmetrical ripple lamination; hummocky cross-stratification with concavo-convex lamination over hummocks and filling troughs	-10 ± 10 m	SP2, PV4
Intertidal Flat (Low-Energy)	fine sandy silt to medium sand; well to very well sorted; symmetrical to fine skewed	muddy beds with ripple lamination, root casts into sand below, flame structures into sand above; sandy beds massive, or with faint ripples, cross-lamination, flaser bedding	0 ± 5 m	Mud: SP3ace, PV3a, PC5b, VP4; Sand: SP3bdf, PV2ac, MN3a
Intertidal Flat (High-Energy)	muddy to pebbly medium sand; moderately to poorly sorted; fine or coarse skewed	massive or variable with ripple lamination, cross-lamination in herringbone sets	0 ± 5 m	MN3bc, MN5, PV3b, PC5a
Colluvial and Cliff-Front Beach	gravelly medium to coarse sand; moderately to poorly sorted; coarse skewed	massive or faint parallel lamination; gravel lenses with imbrication dipping seaward	>0 m	SP4, PV1b, MN4, FG2ab, VP2ab, VF2ab
Upland Fluvial	gravelly medium to coarse sand; poorly sorted; symmetrical to fine skewed	gravel lag, imbricated; fining upwards to muddy or peaty capping unit	>10 m	PC2

a relatively steep coastal margin attests to strong base-level control on their formation. This is further supported in some cases by geomorphic evidence such as wave-cut notches and nearly level bedrock platforms. Finally, pollen assemblages dominated by coastal heath and remains of common reed and sedges recovered from some units indicate a beach, foredune, lagoon, or estuarine setting.

Sedimentological and morphological evidence was useful in determining facies associations for various structureless units in the study area (Table 4), including massive sands and pebbly sands that occur on tidal flats, colluvial slopes, and may also occur in shallow aquatic environments. Many of the sandy units have particle size parameters that fall within the typical range of both modern tidal flat and modern aeolian deposits. We interpret these massive sands as low-energy tidal flats in cases where they are capped by muddy ripple-laminated beds that contain root traces consistent with the growth of marsh grasses (PV3, MN3, PC5). In other cases they are capped with a well-developed paleosol indicating a colluvial/terrestrial origin (VP2). Structureless pebbly units at the base of the Holocene dunes are also considered to be colluvial in origin (PV1b). Sandy and pebbly units with hummocky cross-stratification (SP2, PV4) are interpreted as shoreface storm deposits following Myrow and Southard (1991), but they are probably from the inner shoreface given their position adjacent to bedrock uplands that parallel the coast. Given the neotectonic activity and historical occurrence of tsunami in the study area, the possibility exists that the bluff units may include tsunami deposits as discussed by Costa (2006) for sediments in the Óbidos lagoon. Unfortunately there is little agreement on diagnostic criteria for tsunami deposits and they cannot be conclusively identified without independent evidence (Dahanayake and Kulasena, 2008).

5.2. Age and correlation of raised beaches

Late Pleistocene coastal deposits in the study area date to MIS 6 (151 ka), MIS 5 or older (>101 ka), the MIS 4–3 transition (62–63 ka), and MIS 3 (47, 39–42, and 34–36 ka). Of these, the younger MIS 3 deposits are the most widespread with good agreement in ages across multiple sites (Fig. 13). The coastal complex with dates centered on 42 ka includes muddy to sandy tidal deposits between São Pedro de Muel and Mira Nascente. Above the 42 ka deposits at each of these sites lies a beach and foreshore complex with dates centered on about 35 ka, in most cases marked by an abrupt boundary that truncates features of the lower beds. The position of these strata relative to sea level at the time of deposition is subject to large uncertainties, but by simple superposition the 35 ka strata represent a rapid relative sea level rise (beach/shoreface over tidal flat) of at least 5 m above the 42 ka deposits. The 62 ka, 42 ka, and 35 ka coastal complexes likely correlate with rapid glacioeustatic sea level fluctuations during MIS 3 that are not yet fully understood. While the original SPECMAP stacked isotopic estimate places eustatic sea level during MIS 3 at 80–100 m below modern (Imbrie et al., 1984), a growing body of work documents relative sea level high stands during MIS 3 that reached levels close to modern (–25 m or less). Examples include south Australia (Cann et al., 2000); the Boso Peninsula of Japan (Kuwabara et al., 1999); the Crotona Peninsula, Italy (Mauz and Hassler, 2000); the Bay of Cadiz, Spain (Gracia et al., 2008); the Mediterranean coast of France (Lambeck and Bard, 2000); the Gulf of Mexico (Simms et al., 2009); and the Outer Banks of North Carolina, USA (Mallinson et al., 2008). In a recent review of eustatic sea level reconstructions, Caputo (2007) demonstrated a wide range of possible high stands during MIS 3 and discussed the inherent difficulties in comparing coastal geologic evidence with eustatic estimates. Siddall et al. (2008) offered an extensive review of eustatic sea level studies for MIS 3,

concluding that most published eustatic reconstructions show 3 or 4 fluctuations of 20–40 m amplitude during the period between 30 and 60 ka. Some of these are reproduced in Fig. 12 to demonstrate their range of variability, including reconstructions derived from coral terraces (Thompson and Goldstein, 2006), benthic foraminifera (Shackleton et al., 2000), and planktic foraminifera (Lea et al., 2002). These and other high-resolution eustatic sea level records show fluctuations during MIS 3 in the range between –20 m and –80 m relative to modern (Chappell and Shackleton, 1986; Linsley, 1996; Siddall et al., 2003). Much of the disagreement between these reconstructions is related to the different time models and synchronization mechanisms employed. Importantly, many studies show the final MIS 3 rise at around 30–40 ka to have reached a level above previous high stands, followed by a dramatic drop to the MIS 2 lowstand (Siddall et al., 2008 and works cited therein). The Estremadura sections dated to MIS 3 tend to support these interpretations.

The dated samples that cluster around 42 ka and 35 ka are separated by Heinrich event 4 (HE4), which has been established as a period of extreme cold, aridity, and forest decline in Iberia at about 39 ka (Sánchez-Goñi et al., 2000; Roucoux et al., 2005; Vautravers and Shackleton, 2006). If these deposits are interpreted as two relative sea level high stands forced by eustatic sea-level change, they may fit into a currently debated paleoceanographic model of phase relationships between North Atlantic climate, ice sheet behavior, and eustatic sea-level change during MIS 3 (MacAyeal, 1993; Hemming, 2004; Siddall et al., 2008). This model holds that episodes of glacioeustatic rise during MIS 3 are driven by ice sheet purging during Heinrich events, following periods of slow ice sheet growth and glacioeustatic fall. The intervals between Heinrich events are marked by 3–4 interstadial (IS) events of decreasing warmth, alternating with stadial events that are cold but less severe than the Heinrich events. The magnitude of eustatic sea level rise that could be produced by this mechanism is on the order of 3–15 m, and their timing would be semi-periodic similar to Bond cycles (Bond et al., 1993; Hemming, 2004). This model is in broad agreement with isotopic evidence from deep-sea sediment records (Shackleton et al., 2000) and coral terrace records (Chappell, 2002). The grouped Estremadura samples at 35 ka and 42 ka occur during the intervals between HE3–4 and HE4–5, in agreement with the notion of eustatic rise and fall in synchronization with the timing of Heinrich events and Bond cycles. Additional evidence for rapid relative sea level rise during Heinrich events could provide further support for the binge-purge model of coupled ice sheet and sea-level change.

5.3. Archaeological significance

The Paleolithic artifacts recovered from uplifted coastal deposits in the study area represent a small but significant advance in the archaeological record of Portugal. The major finds include Middle Paleolithic artifacts of the Mousterian type, indicative of Neanderthal populations, at Mira Nascente and Praia Rei Cortiço. At Mira Nascente these artifacts were found in a pebbly sand deposit dated to 40–42 ka (MN3); at Praia Rei Cortiço they were in a similar pebbly sand (PC5) that has not yet been directly dated, but underlies an aeolian sand dated to 101 ka (PC4). We interpret both of these as intertidal flats on the basis of sedimentology, paleotopography, and stratigraphic association with beach deposits as described above (Table 4). In the case of Mira Nascente, the archaeological unit traces laterally to the north into a mud-draped tidal flat deposit at Polvoeira (PV3a), and to the south into an organic-rich paleochannel fill (MN3c). In the case of Praia Rei Cortiço, the artifacts were recovered from the surface of a muddy sand deposit on the margin of a paleochannel, in close proximity to a thick organic bog deposit (PC5c, as yet undated). Other

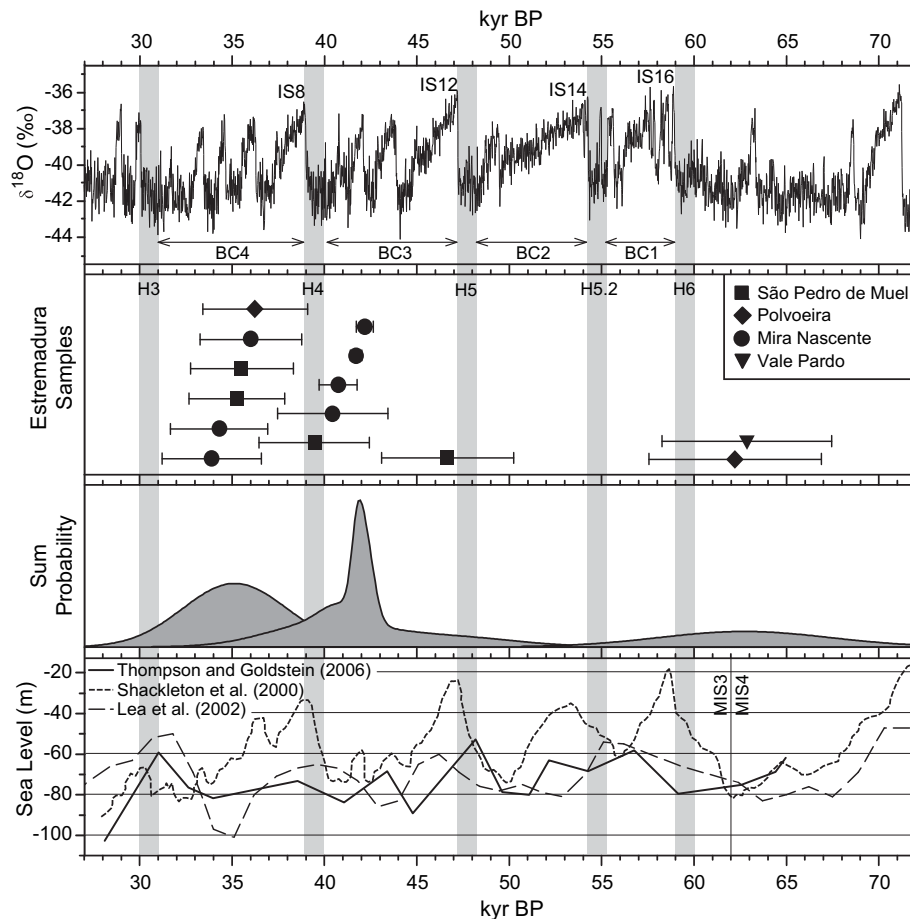


Fig. 13. Correlations between the Greenland ice core climate proxy record, age of Estremadura coastal samples, and sea level reconstructions for MIS 3. (a) GRIP oxygen isotope record plotted on the SFCP timescale of Shackleton et al. (2004). Greenland interstadials (IS), Heinrich Events (H), and Bond Cycles (BC) are numbered for reference. (b) OSL and radiocarbon age and error range for samples from intertidal and shoreface units in this study. (c) Sum of probability distributions for sample groups centered at 35 ka, 42 ka, 62 ka. (d) Selected sea level reconstructions demonstrating variability in timing and magnitude of fluctuations during MIS 3.

archaeological sites in the study area contain lithic assemblages of similar age, establishing Portuguese Estremadura as a promising location to investigate the role of coastal environments during the Middle–Upper Paleolithic transition (Haws et al., 2009).

While Neanderthal adaptation to coastal environments is a hotly-debated topic, the discovery of Middle Paleolithic artifacts in a tidal flat or coastal setting is extraordinarily rare due to the inundation of most coastlines by postglacial sea level rise (Erlandson and Fitzpatrick, 2006; Westley and Dix, 2006). Exceptions exist in areas of rapid neotectonic uplift and along coastlines with steep offshore bathymetry, both of which can be found on the Iberian Peninsula (Bicho and Haws, 2008). Several cave sites in Portugal and Spain include Pleistocene occupations with preserved remains of marine mammals, fish, mollusks, crustaceans and shore birds. These include Figueira Brava in Portugal (Antunes, 2000a,b), Gorham's and Vanguard Caves in Gibraltar (Finlayson et al., 2006, 2008; Stringer et al., 2008), and Cueva de Nerja in Spain (Cortes-Sanchez et al., 2008). Open-air sites such as Mira Nascente and Praia Rei Cortiço typically do not have preserved faunal remains, or lack datable materials, and thus have often been ignored in considerations of coastal adaptations. The archaeological evidence presented here shows that detailed geomorphic and stratigraphic analysis, together with improved age control, can increase the value of open-air sites even in the absence of faunal preservation. This landscape approach is emerging as a promising frontier in geoarchaeology that can augment the traditional site-based approach for exploring patterns of human settlement and resource use (Fanning et al., 2009).

The chief importance of sites like Mira Nascente and Praia Rei Cortiço rests in the identification of Neanderthal use of particular landscapes, in this case, coastal wetlands. Previously, sites in Portugal have been found exclusively in caves or in fluvial depositional settings (Bicho and Haws, 2008). This represents an inherent bias in the Middle Paleolithic archaeological record that limits the range of hypotheses that can be tested about Neanderthal ecology. Furthermore, cave and floodplain sites are typically cumulative palimpsests of multiple occupations over long periods of formation, containing thousands of artifacts. In contrast, Mira Nascente and Praia Rei Cortiço contain limited material remains accumulated over brief moments in time. Stratigraphic mapping and refit analysis for Mira Nascente suggest at least three occupations during the formation of unit MN3 (42–40 ka), with the largest artifact concentration being deposited during one episode of activity (Haws et al., 2009). While these sites are not as informative as sites with large artifact assemblages and faunal preservation, they demonstrate a recurrent pattern of coastal wetland occupation in Portuguese Estremadura. This evidence supports a developing hypothesis that Neanderthal exploitation of the coastal eco-niche in Portugal may have enabled their late survival here (Hockett and Haws, 2005; Stringer et al., 2008).

5.4. Geomorphic response to sea-level and climate change

The stratigraphic units that post-date HE3 suggest subaerial exposure and colluvial deposition on the coastal bluffs during the

Table 5
High, low, and central estimates for uplift rates of Pleistocene beach complexes.

Age of beach complex	Stratigraphic unit	Modern elevation (m) ^a			Elevation when deposited (m) ^b			AMS radiocarbon or OSL age (ka) ^c			Uplift rate (mm yr ⁻¹) ^d		
		High	Low	Central	High	Low	Central	High	Low	Central	High	Low	Central
35 ka	SP2, 3b	26.0	17.1	21.8	-100	-15	-40	30.1	41.1	35.3	4.2	0.8	1.8
	PV2a,b,c	25.8	21.8	22.0	-85	-15	-40	30.6	41.9	36.3	3.6	0.9	1.7
	MN2	42.0	32.2	37.5	-80	-10	-35	28.6	41.5	36.0	4.3	1.0	2.0
42 ka	SP3d	16.8	15.3	16.5	-85	-15	-40	33.5	45.4	39.5	3.0	0.7	1.4
	MN3a,b	32.2	30.6	32.0	-85	-15	-40	34.5	46.4	40.5	3.4	1.0	1.7
62 ka	PV4	19.8	12.0	19.0	-100	-20	-50	52.9	71.5	62.2	2.3	0.4	1.1
	VP3a	57.5	52.5	55.0	-80	-10	-35	53.7	72.0	62.9	2.6	0.9	1.4

^a Elevation of dated stratigraphic units based on field survey: high estimate = top of strata; low estimate = bottom of strata; central estimate = elevation of dated sample.

^b Elevation of dated strata below modern sea level when deposited, based on altitude of deposits relative to sea level (Table 4), added to assumed eustatic levels of MIS3 high stands: high estimate = -80 m, low estimate = -20 m, central estimate = -40 m.

^c Age estimates for dated strata (Tables 1 and 2): high estimate = minimum sample age - 2σ; low estimate = maximum sample age + 2σ; central estimate = central age for sample used in central elevation estimate.

^d Apparent uplift rate for each scenario determined by (Rate) = (Modern Elevation - Elevation When Deposited)/(Age). Uplift rates reflect the net effects of tectonic, halokinetic, and isostatic processes.

relative sea level low stands of MIS 3–2, followed by stabilization and soil formation during MIS 1. Similar “paraglacial” colluvial sections are exposed in eroding coastal bluffs along the Galician coast of northwestern Spain (Blanco Chao et al., 2002; Alonso and Pagés, 2007). The notion of strong upland erosion and landscape instability beginning around the time of HE3 matches colluvial, aeolian, and fluvial evidence from inland parts of Estremadura (Benedetti et al., 2009). This evidence includes truncated soil profiles and stone lines at the base of the Holocene dunes, OSL ages on the base of the inland dune field near Fanheis (13 ka, 27 ka), and the ages of fluvial valley fills from the Rio Tornada valley (31 ka) and from Praia Rei Cortico unit PC2 (15 ka). The upper peat deposit at Praia Rei Cortico (5 ka), together with buried soils in the Holocene dune belt (1.9–2.7 ka), record climatic amelioration and stabilization of the landscape during the Middle Holocene. Ample evidence exists for aeolian reactivation and dune field expansion along the Iberian Atlantic margin during historical times, especially during the Medieval period and again during the Little Ice Age (Granja and Carvalho, 1992; Borja et al., 1999; Clarke and Rendell, 2006; Danielson, 2008; Granja et al., 2008).

5.5. Tectonic history

Relative sea-level change along a given coastal section is the result of eustatic, tectonic, and isostatic factors. Under ideal conditions, the relative impacts of these components can be determined by comparison with regional sea level index points and isostatic modeling. Lambeck et al. (2004) were able to isolate tectonic, eustatic, and isostatic components of relative sea-level change in Italy for the Holocene, and have applied similar methods elsewhere in the Mediterranean (Lambeck, 1995; Lambeck and Bard, 2000). Their methods include comparison with nearby control points of known tectonic stability, and on glacio-hydro-isostatic models calibrated to independent evidence of ice sheet decay and mantle rheology. These conditions cannot currently be met for the Portuguese coast for MIS 3. There are no agreed-upon eustatic sea level control points on the Iberian margin, and little agreement on ice sheet dynamics from which to predict isostatic adjustments. For the Italian coast, Lambeck et al. (2004) found that the eustatic component is dominant but that isostatic adjustments are also significant. Some geophysical studies have demonstrated high mantle viscosity on the Portuguese margin (Brun and Beslier, 1996; Cloetingh et al., 2005), which may limit the magnitude of isostatic response in this area.

The Pleistocene beach deposits dated to MIS 3 (35–62 ka) are found at elevations of 12–58 m above modern sea level. Given the widely accepted depression of eustatic sea level during the last glacial stage, these deposits have clearly been uplifted by some combination of regional compressive stresses, salt tectonics, and isostatic adjustments. These processes are extremely complex in the study area and likely include variable thrusting and tilting of fault blocks, wrenching and transpression along the Nazaré fault, and regional halokinesis as well as development of localized salt domes (Rasmussen et al., 1998). Since these dynamics are only partially understood, their relative contribution to Quaternary uplift rates cannot presently be untangled. As discussed above, large uncertainties also surround the question of eustatic sea level at the time these deposits were emplaced. However, starting with assumptions about eustatic sea level high stands during MIS 3, apparent uplift rates for the Estremadura coast (incorporating both eustatic and isostatic components) can be reasonably well-constrained (Table 5). These calculations clearly demonstrate the importance of tectonic displacement of Pleistocene shorelines in central Portugal, a factor that has been discounted in some previous investigations (Rodrigues et al., 1991; Dias et al., 2000).

Estimated uplift rates in Table 5 are based on assumptions about the elevation reached by eustatic sea level high stands during MIS 3 (discussed above), the elevation relative to sea level at which the sediments were deposited (Table 4), and the accuracy of the age estimates (Tables 1 and 2). We have incorporated a generous error range for each of these assumptions in determining a high, low, and central estimate of uplift for the three Estremadura beach complexes that have multiple dated sections. The dominant source of uncertainty in these calculations is the elevation at which the deposits were originally emplaced, which varies between -10 and -95 m depending on the eustatic sea level estimate chosen and the assumed position of the deposits relative to that level. Potential isostatic adjustments are not considered separately in these calculations, but in this unglaciated region they can be considered small in comparison with the range of possible eustatic sea levels.

The central estimates broadly converge on uplift rates of 1–2 mm yr⁻¹, based on an assumed eustatic level of about -40 m during MIS 3 high stands. The highest and lowest estimates for uplift rates differ by a factor of about 3–5. These uplift rates are rapid enough that they probably cannot be accounted for by regional tectonic stresses and isostasy alone. Most of the uplift is likely related to localized salt tectonics, particularly uplift of the Caldas da Rainha and São Pedro de Muel diapirs. Additional research is necessary to establish geographic relationships between

the diapiric structures that intersect the Estremadura coastline, the uplift rates associated with them, and the sites where Pleistocene raised beaches are preserved. If uplift rates of 1–2 mm yr⁻¹ apply broadly to coastal bluffs in the study area, then the coastal terrace at Cafurno (20–30 m elevation) and the beach deposits at Praia Rei Cortiço (PC3, 12–18 m) may be tentatively assigned to MIS 3. Shorelines of the Last Interglacial (MIS 5e) should have been uplifted to elevations of more than 100 m, and this evidence has likely been lost to erosion.

Uplift rates reported here for emerged MIS 3 coastal deposits are considerably higher than those reported for inland parts of central Portugal where salt tectonics play little or no role. For example, an average rate of 0.1 mm yr⁻¹ was reported for Quaternary uplift in the Tejo valley by Cunha et al. (2005), and 0.2 mm yr⁻¹ uplift in central Portugal since the beginning of the Pliocene by Cloetingh et al. (2005). We are not aware of previous attempts to constrain uplift rates for the central Portuguese coast, but several recent studies show that localized uplift of the magnitude reported here is not unprecedented for the Iberian margin. For example, Gracia et al. (2008) cite 25 m of uplift for an MIS 3 beach deposit dating to 31.5 ka in the Bay of Cadiz, on the Atlantic coast of SW Spain. This would yield an uplift rate of about 0.8 mm yr⁻¹, or greater if MIS 3 eustatic sea level is assumed to have been below –30 m relative to modern. They attribute this uplift to diapiric activity, concluding that such rapid rates could not be explained by the regional tectonic setting. In northwestern Portugal, Carvalho et al. (2006) report an MIS 3 age for beach gravels in the Cepães Formation at modern elevations of up to 6 m. This suggests at least 25 m of uplift, with rates approaching 1 mm yr⁻¹ if MIS 3 eustatic sea level was assumed to be at least 20 m below modern. Granja and De Groot (1996) presented evidence of a Holocene lagoon deposit at Corte-gaça Beach in northwestern Portugal that was raised by as much as 15 m in the past 6 ka, giving an uplift rate of up to 2.5 mm yr⁻¹.

6. Conclusions

Uplifted beach and coastal deposits from northern Estremadura contain evidence of relative sea-level change, geomorphic response, and human occupation of the coastal zone during the last glacial stage. Three sets of coastal deposits from MIS 3 are preserved with OSL ages centered at 62 ka, 42 ka, and 35 ka. Evidence for the coastal origin of these deposits includes sedimentary structures that suggest an intertidal or shoreface origin, geomorphic features such as raised bedrock platforms and wave-cut notches, and botanical remains such as reed fragments and pollen of common coastal taxa. These deposits record local relative sea level fluctuations that were forced by eustatic sea level rise and fall driven by changes in global ice volume during MIS 3. A connection with the timing of Heinrich Events seems likely, as HE4 occurred during the gap between the two younger beach complexes. Dated sections from the coastal bluffs and inland settings suggest widespread upland erosion and fluvial, colluvial, and aeolian deposition beginning around the time of HE3, and continuing through the glacial maximum, followed by stabilization and soil formation in the Holocene. Middle Paleolithic archaeological sites are found in association with tidal flat and paleo-channel deposits in two locations, with ages of about 42 ka (Mira Nascente) and >101 ka (Praia Rei Cortiço). These sites confirm Neanderthal occupation of the coastal niche, although without faunal preservation their use of marine resources is uncertain. Additional Upper Paleolithic sites suggest a low density of anatomically modern humans in the area after about 25 ka. The chronology established here is a first step towards establishing the local response to climatic and environmental changes recorded in

ice cores, deep-sea sediments, and pollen records from around the North Atlantic region.

Perhaps the most significant finding of this study is the estimate of Late Quaternary uplift rates of about 1–2 mm yr⁻¹ for dated sections of the Estremaduran coast. These rates are based on the ages and modern elevations of coastal deposits with an intertidal origin, combined with broad estimates of eustatic sea level during MIS 3. Rapid coastal uplift appears to be highly localized and is related to the complex tectonic setting of the area. Several active diapirs probably account for the order-of-magnitude discrepancy between estimates of local uplift rates for the coastal sections described here and those that prevail in the interior of central Portugal (0.1–0.2 mm yr⁻¹). Rapid uplift of coastal bluffs on the flanks of the São Pedro de Muel and Caldas da Rainha diapirs has been essential in preserving and exposing geological and archaeological evidence of MIS 3 coastal environments in this area. While some previous studies provide corroborative evidence for rapid uplift along parts of the Portuguese margin, this is the first attempt to quantify Late Quaternary uplift rates for the central coast of Portugal. Data from the raised beaches provide a valuable complement to existing paleoenvironmental information for MIS 3 in central Portugal, which mostly comes from offshore sediment cores, archaeological sites, and fluvial terraces in the Tejo valley. Future work in this area will help to establish age control for additional raised beach sections, delineating their full areal extent and precise relationship to tectonic features.

Acknowledgements

This project was supported primarily by the National Science Foundation Archaeology Program (BCS-1455145; BCS-0715279). The lead author was supported by a Charles L. Cahill Award, Faculty Reassignment Award, and International Travel Awards from the University of North Carolina Wilmington. Pollen analyses for São Pedro de Muel and Mira Nascente were performed by Marjeta Jeraj, Department of Botany, University of Wisconsin, Madison. The authors are indebted to Carlos Mendonça, president of ADEPA (Associação para a Defesa e Valorização do Património de Alcobaça) for logistical support. We thank the Portuguese Ministry of Culture, Institute of Archaeology, and Geographic Institute for permits and access to data. We also wish to thank student field and laboratory assistants from the University of Louisville, University of North Carolina Wilmington, Richard Stockton College, and Universidade do Algarve. Finally, we thank Mark Siddall and an anonymous reviewer for helpful comments that improved the paper significantly.

References

- Abrantes, F., Lebreiro, S., Rodrigues, T., Gil, I., Bartels-Jónsdóttir, H., Oliveira, P., Kissel, C., Grimalt, J.O., 2005. Shallow-marine sediment cores record climate variability and earthquake activity off Lisbon (Portugal) for the last 2000 years. *Quaternary Science Reviews* 24, 2477–2494.
- de Abreu, L., Shackleton, N.J., Schönfeld, J., Hall, M., Chapman, M.R., 2003. Millennial-scale oceanic climate variability off the western Iberian margin during the last two glacial periods. *Marine Geology* 196, 1–20.
- Alonso, A., Pagés, J.L., 2007. Stratigraphy of Late Pleistocene coastal deposits in northern Spain. *Journal of Iberian Geology* 33, 207–220.
- Alves, T.M., Manuppella, G., Gawthorpe, R.L., Hunt, D.W., Monteiro, J.H., 2003. The depositional evolution of diapir- and fault-bounded rift basins: examples from the Lusitanian Basin of West Iberia. *Sedimentary Geology* 162, 273–303.
- van Andel, T.H., 2002. Reconstructing climate and landscape of the middle part of the last glaciation in Europe – The Stage 3 Project. *Quaternary Research* 57, 2–8.
- van Andel, T.H., Tzedakis, P.C., 1996. Palaeolithic landscapes of Europe and environs, 150,000–25,000 years ago: an overview. *Quaternary Science Reviews* 15, 481–500.
- Antunes, M., 2000a. The Pleistocene fauna from Gruta da Figueira Brava: a synthesis. *Memórias da Academia das Ciências de Lisboa. Classe de Ciências* 38, 259–282.

- Antunes, M., 2000b. Gruta da Figueira Brava: Pleistocene marine mammals. *Memórias da Academia das Ciências de Lisboa. Classe de Ciências* 38, 245–258.
- Araujo, M.A., Gomes, A., Chamine, H.I., Fonseca, P.E., Gama Pereira, L.C., Pinto de Jesus, A., 2003. Geomorfologia e geologia regional do sector de Porto-Espinho (W de Portugal): implicações morfoestruturais na cobertura sedimentar cenozoica. *Cadernos do Laboratório Xeológico de Laxe* 28, 79–105.
- Aubry, T., Cunha-Ribeiro, J.P., Angelucci, D., 2005. Testemunhos da ocupação pelo Homem de Neanderthal: o sítio da Praia do Pedrógão. In: Carvalho, S. (Ed.), *Habitantes e Habitats: Pré e Proto-História na Bacia do Lis. Saneamento Integrado dos Municípios do Lis (SIMLIS)*, Leiria, Portugal, pp. 56–66.
- Azereido, A.C., Wright, V.P., Ramalho, M.M., 2002. The Middle–Late Jurassic forced regression and disconformity in central Portugal: eustatic, tectonic and climatic effects on a carbonate ramp system. *Sedimentology* 49, 1339–1370.
- Barron, E., Pollard, D., 2002. High-resolution climate simulations of Oxygen Isotope Stage 3 in Europe. *Quaternary Research* 58, 296–309.
- Bender, M.L., Sowers, T., Dickson, M.L., Orchado, J., Grootes, P., Mayewski, P.A., Meese, D.A., 1994. Climate connection between Greenland and Antarctica during the last 100,000 years. *Nature* 372, 663–666.
- Benedetti, M.M., Haws, J.A., Funk, C.L., Daniels, J.M., Hesp, P.A., Bicho, N.F., Minckley, T.A., Ellwood, B.B., Forman, S.L., 2009. Late Quaternary landscapes and seascapes of Portuguese Estremadura: geomorphic response to environmental change during MIS 3 and 2. *Livro de Resúmenes, VII Reunião do Quaternário Ibérico*. Universidade do Algarve, Faro, Portugal, October 2009, pp. 79–82.
- Bicho, N.F., 1993. Late glacial prehistory of central and southern Portugal. *Antiquity* 67, 761–775.
- Bicho, N.F., Haws, J.A., 2008. At the land's end: marine resources and the importance of fluctuations in the coastline in the prehistoric hunter-gatherer economy of Portugal. *Quaternary Science Reviews* 27, 2166–2175.
- Blanco Chao, R.B., Casais, M.C., Cortizas, A.M., Albertia, A.P., Paza, M.V., 2002. Holocene evolution on Galician coast (NW Spain): an example of paraglacial dynamics. *Quaternary International* 93, 149–159.
- Blockley, S.P.E., Ramsey, C.B., Higham, T.F.G., 2008. The Middle to Upper Paleolithic transition: dating, stratigraphy, and isochronous markers. *Journal of Human Evolution* 55, 764–771.
- Blott, S.J., Pye, K., 2001. GRADISTAT: a grain size distribution and statistics package for the analysis of unconsolidated sediments. *Earth Surface Processes and Landforms* 26, 1237–1248.
- Bond, G., Broecker, W., Johnsen, S., McManus, J., Labeyrie, L., Jouzel, J., Bonani, G., 1993. Correlations between climate records from North Atlantic sediments and Greenland ice. *Nature* 365, 143–147.
- Borja, F., Zazo, C., Dabrio, C.J., Diaz del Olmo, F., Goy, J.L., Lario, J., 1999. Holocene aeolian phases and human settlements along the Atlantic coast of southern Spain. *The Holocene* 9, 333–339.
- Boski, T., Moura, D., Veiga-Pires, C., Camacho, S., Duarte, D., Scott, D.B., Fernandes, S.G., 2002. Postglacial sea-level rise and sedimentary response in the Gadiana Estuary, Portugal/Spain border. *Sedimentary Geology* 150, 103–122.
- Breuil, H.M., Zbyszewski, G., 1945. Contribution à l'étude des industries paléolithiques du Portugal et de leurs rapports avec la géologie du Quaternaire: Les principaux gisements des plages quaternaires du littoral d'Estremadura et de terrasses fluviales de la basse vallée du Tage. *Comunicações dos Serviços Geológicos de Portugal* XXVI, 1–662.
- Briant, R.M., Bateman, M.D., 2009. Luminescence dating indicates radiocarbon age underestimation in late Pleistocene fluvial deposits from eastern England. *Journal of Quaternary Science*. doi:10.1002/jqs.1258.
- Brun, J.P., Beslier, M.O., 1996. Mantle exhumation at passive margins. *Earth and Planetary Science Letters* 142, 161–173.
- Cabral, M.C., Freitas, M.C., Andrade, C., Cruces, A., 2006. Coastal evolution and Holocene ostracods in Melides lagoon (SW Portugal). *Marine Micropaleontology* 60, 181–204.
- Cabral, I., Ribeiro, A., 1989. Carta Neotectónica de Portugal na escala 1:1,000,000, Notícia Explicativa. *Serviços Geológicos de Portugal*, Lisboa.
- Cann, J.H., Belperio, A.P., Murray-Wallace, C.V., 2000. Late Quaternary paleosealevels and paleoenvironments inferred from foraminifera, northern Spencer Gulf, south Australia. *Journal of Foraminiferal Research* 30, 29–53.
- Caputo, R., 2007. Sea-level curves: perplexities of an end-user in morphotectonic applications. *Global and Planetary Change* 57, 417–423.
- Carvalho, G.S., Granja, H.M., Loureiro, E., Henriques, R., 2006. Late Pleistocene and Holocene environmental changes in the coastal zone of northwestern Portugal. *Journal of Quaternary Science* 21, 859–877.
- Chappell, J., 2002. Sea level changes forced ice breakouts in the Last Glacial cycle: new results from coral terraces. *Quaternary Science Reviews* 21, 1229–1240.
- Chappell, J., Omura, A., Esat, T., McCulloch, M., Pandolfi, J., Ota, Y., Pillans, B., 1996. Reconciliation of late Quaternary sea levels derived from coral terraces at Huon Peninsula with deep sea oxygen isotope records. *Earth and Planetary Science Letters* 141, 227–236.
- Chappell, J., Shackleton, N.J., 1986. Oxygen isotopes and sea level. *Nature* 324, 137–140.
- Clarke, M.L., Rendell, H.M., 2006. Effects of storminess, sand supply, and the North Atlantic Oscillation on sand invasion and coastal dune accretion in western Portugal. *The Holocene* 16, 341–355.
- Clemmensen, L.B., Lisborg, T., Fornós, J.J., Bromley, R.G., 2001. Cliff-front aeolian and colluvial deposits, Mallorca, Western Mediterranean: a record of climatic and environmental change during the last glacial period. *Bulletin of the Geological Society of Denmark* 48, 217–232.
- Cloetingh, S., Ziegler, P.A., Beekman, F., Andriessena, P.A.M., Matenco, L., Badaa, G., Garcia-Castellanos, D., Hardebola, N., De'zesb, P., Sokoutisa, D., 2005. Lithospheric memory, state of stress and rheology: neotectonic controls on Europe's intraplate continental topography. *Quaternary Science Reviews* 24, 241–304.
- Cortes-Sanchez, M., Morales-Muñiz, A., Simon-Vallejo, M.D., Bergada-Zapata, M.M., Delgado-Huertas, A., Lopez-García, P., Lopez-Saez, J.A., Lozano-Francisco, M.C., Riquelme-Cantal, J.A., Roselló-Izquierdo, E., Sanchez-Marco, A., Vera-Pelaez, J.L., 2008. Palaeoenvironmental and cultural dynamics of the coast of Málaga (Andalusia, Spain) during the Upper Pleistocene and early Holocene. *Quaternary Science Reviews* 27, 2176–2193.
- Costa, P., 2006. Geological recognition of abrupt marine invasions in two coastal areas of Portugal. Unpublished master's thesis, Brunel University, Uxbridge, UK.
- Cunha, P.P., Martins, A.A., Daveau, S., Friend, P.F., 2005. Tectonic control of the Tejo river fluvial incision during the late Cenozoic in Ródão – central Portugal (Atlantic Iberian border). *Geomorphology* 64, 271–298.
- Cunha, P.P., Martins, A.A., Huot, S., Murray, A., Raposo, L., 2008. Dating the Tejo river lower terraces in the Ródão area (Portugal) to assess the role of tectonics and uplift. *Geomorphology* 102, 43–54.
- Dahanayake, K., Kulasena, N., 2008. Recognition of diagnostic criteria for recent- and paleo-tsunami sediments from Sri Lanka. *Marine Geology* 254, 180–186.
- Daniau, A.L., Sánchez-Gofñi, M.F., Beaufort, L., Laggoun-Défarge, F., Loutree, M.F., Duprat, J., 2007. Dansgaard-Oeschger climatic variability revealed by fire emissions in southwestern Iberia. *Quaternary Science Reviews* 26, 1369–1383.
- Danielson, R., 2008. Palaeoecological development of the Quiaios-Mira dunes, northern-central littoral Portugal. *Review of Palaeobotany and Palynology* 152, 74–99.
- Dansgaard, W., Johnsen, S.J., Clausen, H.B., Dahl, J., Gundestrup, N.S., Hommer, C.U., Huidberg, C.S., Steffensen, J.P., Svernbjornsdottir, A.E., Jouzel, J., Bond, G., 1993. Evidence for general instability of past climate from a 250 kyr ice-core record. *Nature* 364, 218–220.
- Dias, R.P., Cabral, J., 2002. Interpretation of recent structures in an area of cryptokarst evolution – neotectonic versus subsidence genesis. *Geodinamica Acta* 15, 233–248.
- Dias, J.M.A., Boski, T., Rodrigues, A., Magalhães, F., 2000. Coast line evolution in Portugal since the Last Glacial Maximum until present – a synthesis. *Marine Geology* 170, 177–186.
- Dinis, J.L., Henriques, V., Freitas, M.C., Andrade, C., Costa, P., 2006. Natural to anthropogenic forcing in the Holocene evolution of three coastal lagoons (Caldas da Rainha valley, western Portugal). *Quaternary International* 150, 41–51.
- Dinis, P., Soares, A.F., Cabral, J., 2007. Genesis of deformation structures affecting Plio-Pleistocene sediments in the western Portuguese mainland (West Iberia). Implication on the regional neotectonics. *Geodinamica Acta* 20, 415–431.
- Diniz, F., 2003. The particular aspect of Pleistocene pollen flora from the west coast of Portugal. Abstract of poster presented at the XVI INQUA Congress, Reno, NV.
- d'Errico, F., Sánchez-Gofñi, M.F., 2003. Neanderthal extinction and the millennial scale climatic variability of OIS 3. *Quaternary Science Reviews* 22, 769–788.
- Ellwood, B.B., Peter, D.E., Balsam, W., Schieber, J., 1995. Magnetic and geochemical variations as indicators of palaeoclimate and archaeological site evolution: examples from 41TR68, Fort Worth, Texas. *Journal of Archaeological Science* 22, 409–415.
- Ellwood, B.B., Crick, R.E., El Hassani, A., Benoist, S., Young, R., 2000. Magneto-susceptibility event and cyclostratigraphy (MSEC) in marine rocks and the question of detrital input versus carbonate productivity. *Geology* 28, 1135–1138.
- Erlanson, J.M., 2001. The archaeology of aquatic adaptation: paradigms for a new millennium. *Journal of Archaeological Research* 9, 287–350.
- Erlanson, J.M., Fitzpatrick, S.M., 2006. Oceans, islands, and coasts: current perspectives on the role of the sea in human prehistory. *Journal of Island and Coastal Archaeology* 1, 5–32.
- Fairbanks, R.G., Mortlock, R.A., Chiu, T.C., Cao, L., Kaplan, A., Guilderson, T.P., Fairbanks, T.W., Bloom, A.L., Grootes, P.M., Nadeau, M.J., 2005. Radiocarbon calibration curve spanning 0 to 50,000 years BP based on paired $^{230}\text{Th}/^{234}\text{U}$ and ^{14}C dates on pristine corals. *Quaternary Science Reviews* 24, 1781–1796.
- Fanning, P.C., Holdaway, S.J., Rhodes, E.J., Bryant, T.G., 2009. The surface archaeological record in arid Australia: geomorphic controls on preservation, exposure, and visibility. *Geoarchaeology* 24, 121–146.
- Ferreira, A.B., 1991. Neotectonics in Northern Portugal: a geomorphological approach. *Zeitschrift für Geomorphologie Supplementband* 82, 73–85.
- Ferreira, O., Dias, J.A., Taborda, R., 2008. Implications of sea-level rise for continental Portugal. *Journal of Coastal Research* 24, 317–324.
- Finlayson, C., 2008. On the importance of coastal areas in the survival of Neanderthal populations during the Late Pleistocene. *Quaternary Science Reviews* 27, 2246–2252.
- Finlayson, C., Giles Pacheco, F., Rodríguez-Vidal, J., Fa, D.A., Gutiérrez López, J.M., Santiago Pérez, A., Finlayson, G., Allué, E., Baena Preysler, J., Cáceres, I., Carrión, J.S., Fernández Jalvo, Y., Gleeed-Owen, C.P., Jiménez Espejo, F., López, P., López Sáez, J.A., Riquelme Cantal, J.A., Sánchez Marco, A., Giles Guzman, F., Brown, K., Fuentes, N., Valarino, C.A., Villalpando, A., Stringer, C.B., Martínez Ruiz, F., Sakamoto, T., 2006. Late survival of Neanderthals at the southernmost extreme of Europe. *Nature* 443, 850–853.
- Finlayson, C., Fa, D.A., Jiménez-Espejo, F., Carrión, J.S., Finlayson, G., Giles-Pacheco, F., Rodríguez-Vidal, J., Stringer, C., Ruiz, F.M., 2008. Gorham's Cave, Gibraltar – the persistence of a Neanderthal population. *Quaternary International* 181, 64–71.
- Firtion, F., Carvalho, G.S., 1952. Les formations détritiques Quaternaires de S. Pedro de Muel, Leiria (Portugal). In: *Memórias e Notícias*, 32. Publicações do Museu e Laboratório Mineralógico e Geológico da Universidade de Coimbra. 8–21.

- Folk, R.L., Ward, W.C., 1957. Brazos River bar: a study in the significance of grain size parameters. *Journal of Sedimentary Petrology* 27, 3–26.
- Forman, S.L., 1999. Infrared and red stimulated luminescence dating of late Quaternary near shore sediments from Spitsbergen, Svalbard. *Arctic, Antarctic, and Alpine Research* 31, 34–49.
- Forman, S.L., Pierson, J., Lepper, K., 2000. Luminescence geochronology. In: Sowers, J.M., Noller, J.S., Lettis, W.R. (Eds.), *Quaternary Geochronology: Methods and Applications*. American Geophysical Union Reference Shelf 4, pp. 157–176.
- França, J.C., Zbyszewski, G., 1963. Carta Geológica de Portugal na Escala de 1/50,000. Notícia Explicativa da Folha 26-B: Alcobça. Serviços Geológicos de Portugal, Lisboa.
- Freitas, M.C., Andrade, C., Rocha, F., Tassinari, C., Munhá, J.M., Cruces, A., Vidinha, J., Silva, C.M., 2003. Lateglacial and Holocene environmental changes in Portuguese coastal lagoons 1: the sedimentological and geochemical records of the Santo André coastal area. *The Holocene* 13, 433–446.
- Gracia, F.J., Rodríguez-Vidal, J., Cáceres, L.M., Belluomini, G., Benavente, J., Alonso, C., 2008. Diapiric uplift of an MIS 3 marine deposit in SW Spain: implications for Late Pleistocene sea level reconstruction and palaeogeography of the Strait of Gibraltar. *Quaternary Science Reviews* 27, 2219–2231.
- Granja, H.M., 1999. Evidence for Late Pleistocene and Holocene sea-level, neotectonic and climate control in the coastal zone of northwest Portugal. *Geologie en Mijnbouw* 77, 233–245.
- Granja, H.M., Carvalho, G.S., 1992. Dunes and Holocene deposits of the coastal zone north of Mondego Cape, Portugal. In: Carter, R.W.G., Curtis, T.G.F., Sheehy-Skeffington, M.J. (Eds.), *Coastal Dunes: Geomorphology, Ecology, and Management for Conservation*. A.A. Balkema, Rotterdam, Netherlands, pp. 43–50.
- Granja, H.M., de Groot, T.A.M., Costa, A.L., 2008. Evidence for Pleistocene wet aeolian dune and interdune accumulation, S. Pedro da Maceda, north-west Portugal. *Sedimentology* 55, 1203–1226.
- Granja, H.M., de Groot, T.A.M., 1996. Sea level rise and neotectonism in a Holocene coastal environment at Cortegaça Beach (NW Portugal) – a case study. *Journal of Coastal Research* 12, 160–170.
- Greenland Ice-Core Project (GRIP) Members, 1993. Climate instability during the Last Interglacial period recorded in the GRIP ice core. *Nature* 364, 203–208.
- Greenland Ice-Core Project (GRIP) Members, 2004. High-resolution record of Northern Hemisphere climate extending into the Last Interglacial period. *Nature* 431, 147–151.
- Groote, P.M., Stuiver, M., White, J.W., Johnsen, S., Jouzel, J., 1993. Comparison of oxygen isotope records from the GISP2 and GRIP Greenland ice cores. *Nature* 366, 552–554.
- Haslett, S.K., 2000. *Coastal Systems*. Routledge, London, UK.
- Haws, J.A., Funk, C.L., Benedetti, M.M., Bicho, N.F., Daniels, J.M., Hockett, B.S., Jeraj, M., 2009. Late Quaternary landscapes and seascapes of Portuguese Estremadura: Middle and Upper Paleolithic settlement. *Proceedings VII Iberian Quaternary Union. Livro de Resúmenes, VII Reunião do Quaternário Ibérico*. Universidade do Algarve, Faro, Portugal, October 2009, pp. 190–192.
- Hemming, S.R., 2004. Heinrich events: massive Late Pleistocene detritus layers of the North Atlantic and their global imprint. *Review of Geophysics* 42, RG1005.
- Henriques, M.V., Dinis, J.L., 2006. Avaliação do enchimento sedimentar holocénico na planície aluvial da Nazaré (Estremadura Portuguesa). *Proceedings X Colóquio Ibérico de Geografia*. Évora, Portugal, pp. 1–16.
- Hockett, B., Haws, J.A., 2005. Nutritional ecology and the human demography of Neanderthal extinction. *Quaternary International* 137, 21–34.
- Huber, C., Leuenberger, M., Spahni, R., Flückiger, J., Schwander, J., Stocker, T.F., Johnsen, S., Landais, A., Jouzel, J., 2006. Isotope calibrated Greenland temperature record over Marine Isotope Stage 3 and its relation to CH₄. *Earth and Planetary Science Letters* 243, 504–519.
- Huntley, B., Alfano, M.J., Allen, J.R.M., Pollard, D., Tzedakis, P.C., de Beaulieu, J.-L., Grüber, E., Watts, B., 2003. European vegetation during Marine Oxygen Isotope Stage-3. *Quaternary Research* 59, 195–212.
- Imbrie, J., Hays, J.D., Martinson, D.G., McIntyre, A., Mix, A.C., Morley, J.J., Pisias, N.G., Prell, W.L., Shackleton, N.J., 1984. The orbital theory of Pleistocene climate: support from a revised chronology of the marine $\delta^{18}O$ record. In: Berger, A.L. (Ed.), *Milankovitch and Climate*, vol. 1. D. Reidel Publishing Company, Norwell, MA, pp. 269–305.
- Jain, M., Botter-Jensen, L., Singhvi, A.K., 2003. Dose evaluation using multiple-aliquot quartz OSL: test of methods and a new protocol for improved accuracy and precision. *Radiation Measurements* 37, 67–80.
- Jiménez-Espejo, F.J., Martínez-Ruiz, F., Finlayson, C., Paytan, A., Sakamoto, T., Ortega-Huertas, M., Finlayson, G., Iijima, K., Gallego-Torres, D., Fa, D., 2007. Climate forcing and Neanderthal extinction in Southern Iberia: insights from a multiproxy marine record. *Quaternary Science Reviews* 26, 836–852.
- Jöris, O., Adler, D.S., 2008. Setting the record straight: toward a systematic chronological understanding of the Middle to Upper Paleolithic boundary in Eurasia. *Journal of Human Evolution* 55, 761–763.
- Kuwabara, T., Kikuchi, T., Suzuki, T., Kiyonaga, J., 1999. Terraces and sea level estimates from Oxygen Isotope Stage 3 in the lower Isumi River basin, Boso Peninsula, central Japan. *Daiyoni-Kenkyu (Quaternary Research)* 38, 313–326.
- Lambeck, K., 1995. Late Pleistocene and Holocene sea-level change in Greece and south-west Turkey: a separation of eustatic, isostatic and tectonic contributions. *Geophysical Journal International* 122, 1022–1044.
- Lambeck, K., Bard, E., 2000. Sea-level change along the French Mediterranean coast since the time of the Last Glacial Maximum. *Earth and Planetary Science Letters* 175, 202–222.
- Lambeck, K., Antonioli, F., Purcell, A., Silenzi, S., 2004. Sea-level change along the Italian coast for the past 10,000 yr. *Quaternary Science Reviews* 23, 1567–1598.
- Lea, D.W., Martin, P.A., Pak, D.K., Spero, H.J., 2002. Reconstructing a 350 ky history of sea level using planktonic Mg/Ca and oxygen isotope records from a Cocos Ridge core. *Quaternary Science Reviews* 21, 283–293.
- Linsley, B.K., 1996. Oxygen isotope evidence of sea level and climatic variations in the Sulu Sea over the past 150,000 years. *Nature* 380, 234–237.
- MacAyeal, D.R., 1993. Binge/purge oscillations of the Laurentide ice sheet as a cause of the North Atlantic's Heinrich Events. *Paleoceanography* 8, 775–784.
- Maldonado, A., Nelson, C.H., 1999. Interaction of tectonic and depositional processes that control the evolution of the Iberian Gulf of Cadiz margin. *Marine Geology* 155, 217–242.
- Mallinson, D., Burdette, K., Mahan, S., Brook, G., 2008. Optically stimulated luminescence age controls on late Pleistocene and Holocene coastal lithosomes, North Carolina, USA. *Quaternary Research* 69, 97–109.
- Mauz, B., Hassler, U., 2000. Luminescence chronology of Late Pleistocene raised beaches in southern Italy: new data of relative sea-level changes. *Marine Geology* 170, 187–203.
- Mayer, J.H., Burr, G.S., Holliday, V.T., 2008. Comparisons and interpretations of charcoal and organic matter radiocarbon ages from buried soils in north-central Colorado, USA. *Radiocarbon* 50, 331–346.
- Meireles, J., Texier, J.P., 2000. Étude morpho-stratigraphique des dépôts littoraux du Minho (NW du Portugal). *Quaternaire* 11, 21–29.
- Myrow, P.M., Southard, J.B., 1991. Combined-flow model for vertical stratification sequences in shallow marine storm-deposited beds. *Journal of Sedimentary Research* 61, 202–210.
- O'Regan, H.J., 2008. The Iberian peninsula – corridor or cul-de-sac? Mammalian faunal change and possible routes of dispersal in the last 2 million years. *Quaternary Science Reviews* 27, 2136–2144.
- Pereira, A.R., Borges, B., Soares, A.M., Santos, A.P., Neves, M., 2007. Coastal palaeoenvironments: a balance between sea level fluctuations and neotectonics. Examples on Portuguese Estremadura. In: Gómez-Pujol, L., Fornós, J.J. (Eds.), *Investigaciones Recientes (2005–2007) en Geomorfología Litoral*, IV Reunión de Geomorfología Litoral. Palma, Mallorca, pp. 175–177.
- Pinheiro, L.M., Wilson, R.C.L., Pena dos Reis, R., Whitmarsh, R.B., Ribeiro, A., 1996. The western Iberia margin: a geophysical and geological overview. In: Whitmarsh, R.B., Sawyer, D.S., Klaus, A., Masson, D.G. (Eds.), *Proceedings of the Ocean Drilling Program, Scientific Results* 149, pp. 3–21.
- Prescott, J.R., Hutton, J.T., 1994. Cosmic ray contributions to dose rates for luminescence and ESR dating: large depths and long-term time variations. *Radiation Measurements* 23, 497–500.
- Raposo, L., 2000. The Middle–Upper Paleolithic transition in Portugal. In: Stringer, C.B., Barton, R.N.E., Finlayson, J.C. (Eds.), *Neanderthals on the Edge*. Oxbow Books, Oxford, UK, pp. 95–110.
- Rasmussen, E.S., Lomholt, S., Andersen, C., Vejbaek, O.V., 1998. Aspects of the structural evolution of the Lusitanian Basin in Portugal and the shelf and slope area offshore Portugal. *Tectonophysics* 300, 199–225.
- Rodrigues, A., Magalhães, F., Dias, J.A., 1991. Evolution of the north Portuguese coast in the last 18,000 years. *Quaternary International* 9, 67–74.
- Rodríguez-Vidal, J., Cáceres, L.M., Finlayson, J.C., Gracia, F.J., Martínez-Aguirre, A., 2004. Neotectonics and shoreline history of the Rock of Gibraltar, southern Iberia. *Quaternary Science Reviews* 23, 2017–2029.
- Rodwell, J.S., 1995. Aquatic Communities, Swamps and Tall-Herb Fens. In: *British Plant Communities*, vol. 4. Cambridge University Press, Cambridge, UK.
- Rohling, E.J., Grant, K., Hemleben, C., Kucera, M., Roberts, A.P., Schmeltzer, I., Schulz, H., Siccha, M., Siddall, M., Trommer, G., 2008. New constraints on the timing and amplitude of sea level fluctuations during early to middle Marine Isotope Stage 3. *Paleoceanography* 23, PA3219. doi:10.1029/2008PA001617.
- Roucoux, K.H., de Abreu, L., Shackleton, N.J., Tzedakis, P.C., 2005. The response of NW Iberian vegetation to North Atlantic climate oscillations during the last 65 kyr. *Quaternary Science Reviews* 24, 1637–1653.
- Sánchez-Goñi, M.F., Eynaud, F., Turon, J.L., Gendreau, S., 2000. European climatic response to millennial-scale climatic changes in the atmosphere-ocean system during the Last Glacial period. *Quaternary Research* 54, 394–403.
- Shackleton, N., Hall, M., Vincent, E., 2000. Phase relationships between millennial-scale events 64000–24000 years ago. *Paleoceanography* 15, 565–569.
- Shackleton, N.J., Fairbanks, R.G., Chiu, T., Parrenin, F., 2004. Absolute calibration of the Greenland time scale: implications for Antarctic time scales and for $\Delta^{14}C$. *Quaternary Science Reviews* 23, 1513–1522.
- Siddall, M., Rohling, E.J., Almogi-Labin, C., Hemleben, C., Meischner, D., Schmeltzer, I., Smeed, D.A., 2003. Sea-level fluctuations during the last glacial cycle. *Nature* 423, 853–858.
- Siddall, M., Rohling, E.J., Thompson, W.G., Waelbroeck, C., 2008. Marine Isotope Stage 3 sea level fluctuations: data synthesis and new outlook. *Reviews of Geophysics* 46, RG4003.
- Simms, A.R., DeWitt, R., Rodriguez, A.B., Lambeck, K., Anderson, J.B., 2009. Revisiting Oxygen Isotope Stage 3 and 5a (MIS 3–5a) sea levels within the northwestern Gulf of Mexico. *Global and Planetary Change* 66, 100–111.
- Stiner, M.C., 2001. Thirty years on the 'Broad Spectrum Revolution' and Paleolithic demography. *Proceedings of the National Academy of Sciences* 98, 6993–6997.
- Straus, L.G., Bicho, N.F., 2000. The Upper Paleolithic settlement of Iberia: first-generation maps. *Antiquity* 74, 553–567.
- Stringer, C.B., Finlayson, J.C., Barton, R.N.E., Fernández-Jalvo, Y., Cáceres, L., Sabin, R.C., Rhodes, E.J., Currant, A.P., Rodríguez-Vidal, J., Giles-Pacheco, F., Riquelme-Cantal, J.A., 2008. Neanderthal exploitation of marine mammals in Gibraltar. *Proceedings of the National Academy of Sciences* 105, 14319–14324.

- Thomas, P.J., Murray, A.S., Granja, H.M., Jain, M., 2008. Optical dating of Late Quaternary coastal deposits in northwestern Portugal. *Journal of Coastal Research* 24, 134–144.
- Thompson, W.G., Goldstein, S.L., 2006. A radiometric calibration of the SPECMAP timescale. *Quaternary Science Reviews* 25, 3207–3215.
- Thomson, J., Nixon, S., Summerhayes, C.P., Rohling, E.J., Schoenfeld, J., Zahn, R., Grootes, P., Abrantes, F., Gaspar, L., Vaquero, S., 2000. Enhanced productivity on the Iberian margin during glacial/interglacial transitions revealed by barium and diatoms. *Journal of the Geological Society of London* 157, 667–677.
- Vautravers, M.J., Shackleton, N.J., 2006. Centennial-scale surface hydrology off Portugal during Marine Isotope Stage 3, insights from planktonic foraminiferal fauna variability. *Paleoceanography* 21, PA3004.
- Walker, M.J.C., Björck, S., Lowe, J.J., 2001. Integration of ice core, marine and terrestrial records (INTIMATE) from around the North Atlantic region: an introduction. *Quaternary Science Reviews* 20, 1160–1174.
- Weninger, B., Jöris, O., 2008. A ^{14}C age calibration curve for the last 60 ka: the Greenland-Hulu U/Th timescale and its impact on understanding the Middle to Upper Paleolithic transition in Western Eurasia. *Journal of Human Evolution* 55, 772–781.
- Westley, K., Dix, J., 2006. Coastal environments and their role in prehistoric migrations. *Journal of Maritime Archaeology* 1, 9–28.
- Whittington, G., Hall, A.M., 2002. The Tolsta Interstadial, Scotland: correlation with D–O cycles GI-8 to GI-5? *Quaternary Science Reviews* 21, 901–915.
- Yim, W.W.S., Huang, G., Chan, L.S., 2004. Magnetic susceptibility study of Late Quaternary inner continental shelf sediments in the Hong Kong SAR, China. *Quaternary International* 117, 41–54.
- Zazo, C., Silva, P.G., Goy, J.L., Hillaire-Marcel, C., Ghaleb, B., Lario, J., Bardají, T., González, A., 1999. Coastal uplift in continental collision plate boundaries: data from the Last Interglacial marine terraces of the Gibraltar Strait area (South Spain). *Tectonophysics* 301, 95–109.
- Zazo, C., Goy, J.L., Dabrio, C.J., Bardají, T., Hillaire-Marcel, C., Ghaleb, B., González-Delgado, J.A., Soler, V., 2003. Pleistocene raised marine terraces of the Spanish Mediterranean and Atlantic coasts: records of coastal uplift, sea-level highstands and climate changes. *Marine Geology* 194, 103–133.
- Zazo, C., Dabrio, C.J., Goy, J.L., Lario, J., Cabero, A., Silva, P.G., Bardají, T., Mercier, N., Borja, F., Roquero, E., 2008. The coastal archives of the last 15 ka in the Atlantic–Mediterranean Spanish linkage area: sea level and climate changes. *Quaternary International* 181, 72–87.
- Zbyszewski, G., 1971. Carta Geológica do Quaternário de Portugal na Escala de 1/1,000,000: Notícia Explicativa. Serviços Geológicos de Portugal, Lisboa.
- Zilhão, J., 2000. Nature and culture in Portugal from 30,000 to 20,000 BP. In: Roeboeks, W., Mussi, M., Svoboda, J., Fennema, K. (Eds.), *Hunters of the Golden Age: The Mid-Upper Paleolithic of Eurasia 30,000–20,000 BP*. Leiden University Press, Leiden, Netherlands, pp. 337–354.
- Zitellini, N., Rovere, M., Terrinha, P., Chierici, F., Matias, L., Bigsets Team, 2004. Neogene through Quaternary tectonic reactivation of SW Iberian passive margin. *Pure and Applied Geophysics* 161, 565–587.